

RESEARCH ARTICLE

Open Access



# Genomes of the dinoflagellate *Polarella glacialis* encode tandemly repeated single-exon genes with adaptive functions

Timothy G. Stephens<sup>1,2</sup>, Raúl A. González-Pech<sup>1,3</sup>, Yuanyuan Cheng<sup>4,5</sup>, Amin R. Mohamed<sup>6</sup>, David W. Burt<sup>7</sup>, Debashish Bhattacharya<sup>8</sup>, Mark A. Ragan<sup>1</sup> and Cheong Xin Chan<sup>1,9,10\*</sup> 

## Abstract

**Background:** Dinoflagellates are taxonomically diverse and ecologically important phytoplankton that are ubiquitously present in marine and freshwater environments. Mostly photosynthetic, dinoflagellates provide the basis of aquatic primary production; most taxa are free-living, while some can form symbiotic and parasitic associations with other organisms. However, knowledge of the molecular mechanisms that underpin the adaptation of these organisms to diverse ecological niches is limited by the scarce availability of genomic data, partly due to their large genome sizes estimated up to 250 Gbp. Currently available dinoflagellate genome data are restricted to Symbiodiniaceae (particularly symbionts of reef-building corals) and parasitic lineages, from taxa that have smaller genome size ranges, while genomic information from more diverse free-living species is still lacking.

**Results:** Here, we present two draft diploid genome assemblies of the free-living dinoflagellate *Polarella glacialis*, isolated from the Arctic and Antarctica. We found that about 68% of the genomes are composed of repetitive sequence, with long terminal repeats likely contributing to intra-species structural divergence and distinct genome sizes (3.0 and 2.7 Gbp). For each genome, guided using full-length transcriptome data, we predicted > 50,000 high-quality protein-coding genes, of which ~40% are in unidirectional gene clusters and ~25% comprise single exons. Multi-genome comparison unveiled genes specific to *P. glacialis* and a common, putatively bacterial origin of ice-binding domains in cold-adapted dinoflagellates.

**Conclusions:** Our results elucidate how selection acts within the context of a complex genome structure to facilitate local adaptation. Because most dinoflagellate genes are constitutively expressed, *Polarella glacialis* has enhanced transcriptional responses via unidirectional, tandem duplication of single-exon genes that encode functions critical to survival in cold, low-light polar environments. These genomes provide a foundational reference for future research on dinoflagellate evolution.

**Keywords:** Dinoflagellates, Genomics, Genome evolution, *Polarella glacialis*, Cold adaptation

\* Correspondence: [c.chan1@uq.edu.au](mailto:c.chan1@uq.edu.au)

<sup>1</sup>Institute for Molecular Bioscience, The University of Queensland, Brisbane, QLD 4072, Australia

<sup>9</sup>School of Chemistry and Molecular Biosciences, The University of Queensland, Brisbane, QLD 4072, Australia

Full list of author information is available at the end of the article



© The Author(s). 2020 **Open Access** This article is licensed under a Creative Commons Attribution 4.0 International License, which permits use, sharing, adaptation, distribution and reproduction in any medium or format, as long as you give appropriate credit to the original author(s) and the source, provide a link to the Creative Commons licence, and indicate if changes were made. The images or other third party material in this article are included in the article's Creative Commons licence, unless indicated otherwise in a credit line to the material. If material is not included in the article's Creative Commons licence and your intended use is not permitted by statutory regulation or exceeds the permitted use, you will need to obtain permission directly from the copyright holder. To view a copy of this licence, visit <http://creativecommons.org/licenses/by/4.0/>. The Creative Commons Public Domain Dedication waiver (<http://creativecommons.org/publicdomain/zero/1.0/>) applies to the data made available in this article, unless otherwise stated in a credit line to the data.

## Background

Dinoflagellates are a species-rich (2270 species in Algae-Base [1]) and anciently diverged (likely Precambrian origin [2]) group of microbial eukaryotes that are ubiquitous in marine and fresh waters. Mostly photosynthetic, dinoflagellates form the base of food webs. They sustain global aquatic ecosystems via primary production and cycling of organic carbon and nitrogen. Some dinoflagellate lineages comprise species that are symbiotic or parasitic. For example, members of the family Symbiodiniaceae are crucial symbionts in corals and other coral reef animals [3, 4], and parasitic dinoflagellates can cause death in economically important crustaceans, such as crabs and lobsters [5]. Most dinoflagellates, however, are free-living. Bloom-forming taxa may cause ‘red tides’, which produce toxins that pose serious human health risks [6]. Some taxa have specialised to inhabit extreme environments, such as those found in the brine channels of polar sea ice [7–10].

Thus far, available genome data of dinoflagellates are largely restricted to symbiotic or parasitic species [11–17]. These lineages were chosen for sequencing because their genomes are relatively small, i.e., 0.12–4.8 Gbp. In comparison, genomes of other free-living dinoflagellates are much larger in size, ranging from ~7 Gbp in the psychrophile *Polarella glacialis* to over 200 Gbp in *Prorocentrum* sp. based on DAPI staining of DNA content [18].

Repeat content has been estimated at >55% in the genome sequences of some free-living dinoflagellates [19, 20]; single-exon genes have also been described [21]. Given that most dinoflagellate lineages are free-living, whole-genome sequences of these taxa are critical to understand the molecular mechanisms that underpin their successful diversification in specialised environmental niches.

*Polarella glacialis*, a psychrophilic (cold-adapted) free-living species, represents an excellent system for genomic studies of dinoflagellates for three reasons. First, it is closely related to Symbiodiniaceae (both in the order Suessiales), the family that contains the coral reef symbionts, e.g. *Symbiodinium* and related genera. Second, *P. glacialis* has been reported only in polar regions. Studying the *P. glacialis* genome can thus provide insights into the molecular mechanisms that underlie the evolutionary transition of dinoflagellates from a free-living to a symbiotic lifestyle and the adaptation to extreme environments. Third, the estimated genome size of *P. glacialis* is still in the smaller range (~7 Gbp [18]) of all dinoflagellate taxa, which presents a technical advantage in terms of allowing efficient genome assembly and gene prediction.

Here, we report draft de novo genome sequences from two *P. glacialis* isolates: CCMP1383 and CCMP2088. The former is a xenic culture, first isolated from brine in the upper sea ice in McMurdo Sound (Ross Sea, Antarctica)

in 1991 [10], and the latter is a xenic culture first isolated from a water sample collected adjacent to ice in northern Baffin Bay in 1998 [22]. These genomes represent the first generated from free-living, psychrophilic dinoflagellates. Incorporating full-length transcriptome data, we investigated gene structure, repeat content, and intra-species genome divergence. Our results reveal a remarkable difference in genome size between these two isolates of the same species and provide evidence of tandemly repeated, single-exon genes in shaping the evolution of dinoflagellate genomes.

## Results

### Genomes of *Polarella glacialis*

Draft genome assemblies for two *Polarella glacialis* isolates (CCMP1383 and CCMP2088) were generated using a combination of Illumina short-read and PacBio long-read data (Table 1 and Additional file 3: Supplementary Table 1). Both genomes are putatively diploid based on their bimodal distributions of *k*-mer counts observed from the sequence data; the distribution for each assembly matches closely (model fit >92%) the standard theoretical diploid model (Fig. 1a and Additional file 2: Supplementary Fig. 1). No reliable haploid representation could be generated (see the ‘Methods’ section). Although we cannot exclude the possibility that our observations may be caused by recent whole-genome duplication and/or extensive genic diversity, diploid life stages and sexual reproduction have been described in other free-living dinoflagellates [23]. These results represent the first diploid genome assemblies reported for any dinoflagellate; we used these assemblies in subsequent analyses. The CCMP1383 assembly had fewer and more-contiguous scaffolds (33,494; N50 length 170 Kbp; Table 1) compared to the CCMP2088 assembly (37,768; N50 length 129 Kbp; Table 1); this is likely a consequence of more long-read data generated for CCMP1383 (see Additional file 3: Supplementary Table 2). Both assemblies are much more contiguous than their corresponding assemblies generated using only short-read data (N50 length <73 Kbp; Additional file 3: Supplementary Table 1). Almost all short-read data (mean 95% for CCMP1383, 93% for CCMP2088) mapped to the corresponding genome assembly (Additional file 3: Supplementary Table 3). For CCMP1383 and CCMP2088, the total diploid assembly sizes are respectively 2.98 Gbp and 2.76 Gbp (Table 1 and Additional file 3: Supplementary Table 1) and are very similar to independent diploid genome size estimates of 3.02 Gbp and 2.65 Gbp (Additional file 3: Supplementary Table 4) for these isolates. These genomes are smaller than previously estimated (~7 Gbp based on staining of total [assumed haploid, but potentially diploid] DNA content [18]). However, they remain larger than those of Symbiodiniaceae [11–15] (haploid; between 1.1 and 1.5 Gbp) and smaller

**Table 1** Assembled genomes of *P. glacialis* compared to representative publicly available dinoflagellate genomes. A more comprehensive summary including all other available genomes is shown in Additional file 3: Supplementary Table 1. Estimated diploid genome size for *P. glacialis* isolates is shown in brackets

	<i>Polarella glacialis</i>		Symbiodiniaceae				Parasitic	
	CCMP1383	CCMP2088	<i>Symbiodinium microadriaticum</i>	<i>Breviolum minutum</i>	<i>Cladocopium goreau</i>	<i>Fugacium kawagutii</i>	<i>Amoebophrya ceratii</i>	<i>Hematodinium</i> sp.
Reference	This study	This study	Aranda et al. [13]	Shoguchi et al. [14]	Liu et al. [12]	Liu et al. [12]	John et al. [16]	Gornik et al. [17]
%G+C	45.91	46.15	50.51	43.46	44.83	45.72	55.92	47.31
Total number of scaffolds	33,494	37,768	9695	21,899	41,289	16,959	2351	869,500
Total assembled bases (Gbp)	2.98	2.76	0.81	0.61	1.03	1.05	0.09	4.77
N50 length of scaffolds (bp)	170,304	129,205	573,512	125,226	98,034	268,823	83,970	17,235
Maximum scaffold length (bp)	2,170,995	1,500,384	3,144,590	810,747	8,337,000	5,159,000	536,776	186,000
Estimated genome size (Gbp)	1.48 (3.02)	1.30 (2.65)	1.10	1.5	1.19	1.07	0.12	4.8

than the 4.8-Gbp genome of the parasitic *Hematodinium* sp. [17] (Table 1 and Additional file 3: Supplementary Table 1). Our results reaffirm the tendency of DNA staining or flow cytometry to overestimate genome sizes of dinoflagellates [11–15], potentially due to the liquid crystal structure of dinoflagellate chromosomes [24]. The number of chromosomes in dinoflagellates remains elusive [23, 25].

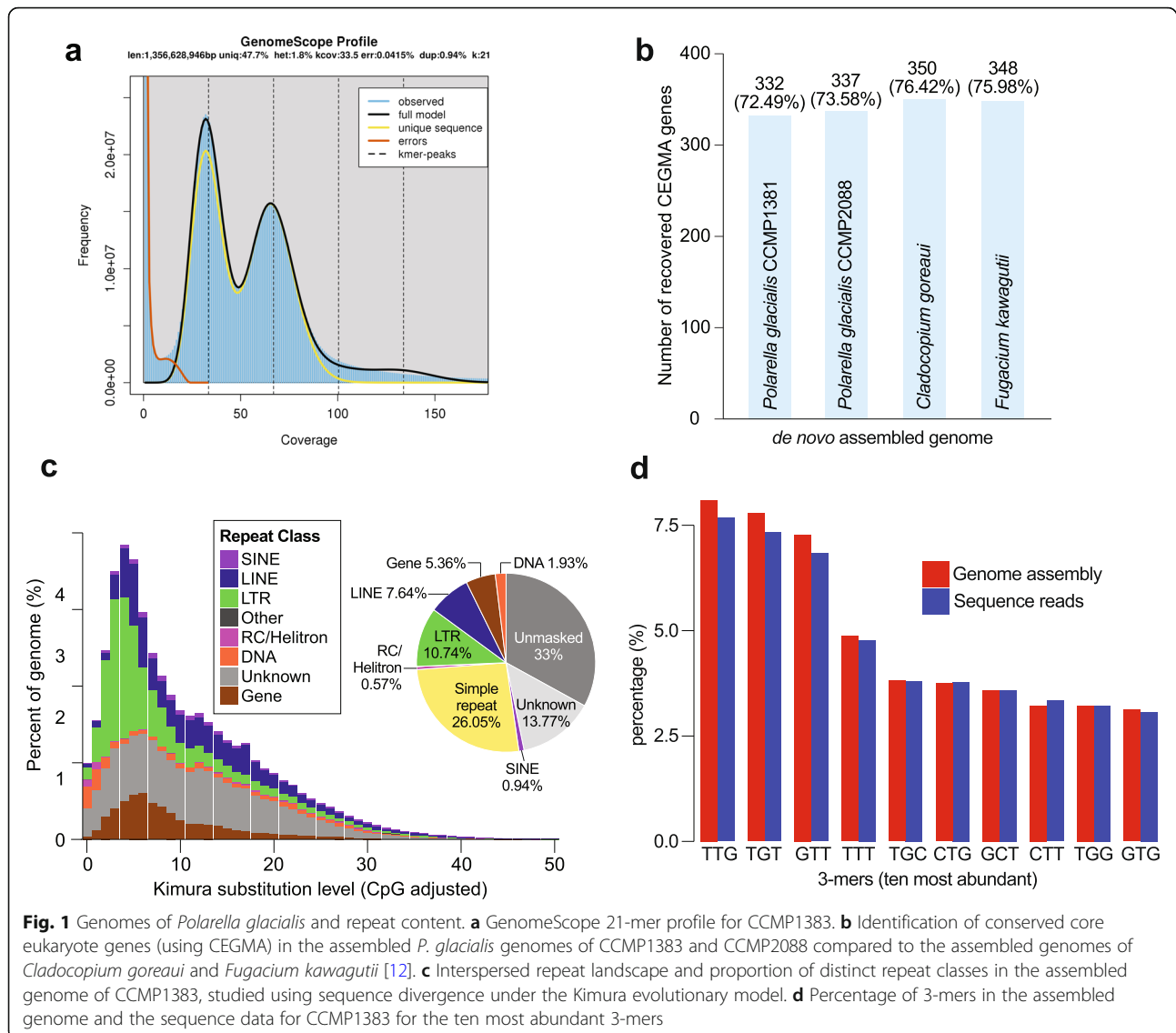
The non-repetitive regions from both assembled genomes are almost identical in content and sequence. In a comparison between the non-repetitive regions of CCMP2088 against the genome of CCMP1383, top hits cover 96.9% of the query bases with an average sequence identity of 99.4%. Likewise, in CCMP1383, top hits cover 95.6% of query bases with an average sequence identity of 99.2% compared against the CCMP2088 genome. Remarkably, the estimated diploid genome size of the Antarctic isolate (CCMP1383) is approximately 370 Mbp larger than that of the Arctic isolate (CCMP2088). These results reveal, for the first time, structural divergence of genomes in dinoflagellates even within a single species, potentially explained by the uneven expansion of repetitive elements (see below). The two genome assemblies are reasonably complete. Similar proportions of core conserved eukaryote genes were recovered, i.e. 332 (72.49%) and 337 (73.58%) of the 458 CEGMA [26] genes in CCMP1383 and CCMP2088, respectively (Fig. 1b and Additional file 3: Supplementary Table 5). These numbers are comparable to those recovered in published symbiodiniacean genomes [12], e.g. 350 in *Cladocopium goreau* and 348 in *Fugacium kawagutii*, analysed using the same approach (Fig. 1b).

The high extent of genome sequence similarity between the two geographically distinct *P. glacialis* isolates suggests that they have either recently been transferred from one polar region to the other or are being actively

transported between the two locations, allowing for mixing of the two populations. To identify if *P. glacialis* is being actively transported between polar regions, we interrogated the TARA Oceans database for the presence of this species in the broadly sampled list of sites. Despite *P. glacialis* sequences being listed in 67 of the 68 TARA sample locations, an exhaustive search based on sequence similarity did not recover clear evidence of any *P. glacialis* sequences (see the ‘Methods’ section). Whereas we cannot dismiss the presence of *P. glacialis* at low, undetectable levels, we find no evidence at this time to support the presence of *P. glacialis* in the waters outside of the polar regions.

#### ***Polarella glacialis* genomes are highly repetitive**

Both *P. glacialis* genomes reveal a high content of repetitive elements that encompass ~68% (by length) of the assembled sequences (Fig. 1c and Additional file 2: Supplementary Fig. 2). Most of these elements are simple and unknown repeats (i.e. unclassified de novo repeats, covering ~13.5% of each assembled genome; Fig. 1c). The proportion of repeats in *P. glacialis* genomes is more than two-fold higher than that reported in Symbiodiniaceae (e.g. 27.9% in *Symbiodinium microadriaticum*, 16% in *Fugacium kawagutii*) [12]. This observation is not unexpected, because even before high-throughput sequencing technology was available, the genome of the biotechnologically important dinoflagellate *Cryptocodinium cohnii* was estimated to contain 55–60% repeat content [19]. A genome survey of *Alexandrium ostenfeldii* estimated the repeat content at ~58% [20]. In comparison, the genome surveys of *Heterocapsa triquetra* [27] and *Prorocentrum minimum* [28] estimated their repeat content at only ~5% and ~6%, respectively. These values are likely underestimates



because only 0.0014% of the *H. triquetra* genome was surveyed, and >28% of the reported *P. minimum* genome data is putatively of bacterial origin [28].

The prevalence of repeats in *P. glacialis* genomes may explain their larger genome sizes compared to symbiotic dinoflagellates [11–15] and may represent a genome signature of free-living dinoflagellates. These repeats are more conserved in *P. glacialis* (Kimura substitution level [29] centred around 5; Fig. 1c and Additional file 2: Supplementary Fig. 2) than those reported in Symbiodiniaceae (Kimura substitution levels 10–30 [12]). We also recovered a substantial proportion of long terminal repeat (LTR) elements (~12%) in *P. glacialis* genomes; these elements were largely absent (<0.7%) in Symbiodiniaceae [12]. Transposable elements (such as LTRs) commonly comprise up to 80% of the genomes of plants and are induced by genome shock and polyploidization,

resulting in genome restructuring [30]. The abundance of LTRs in *P. glacialis* and the role of LTRs in genome restructuring may explain in part the difference in genome sizes between the two isolates. These results suggest that repetitive elements and LTRs are key contributors that drive genome size evolution of *P. glacialis*, both as a free-living and a cold-adapted dinoflagellate species. Because available dinoflagellate genomes (e.g. of Symbiodiniaceae) thus far have been generated largely using Illumina short-read data, we cannot dismiss the possibility that mis-assembly (an inevitable artefact with short-read data) may have caused the under-estimation of repeat content (and the apparent absence of LTRs) in these genomes.

In an independent analysis of simple repeats (see the ‘Methods’ section), 25.01% and 24.17% of the CCMP1383 and CCMP2088 genomes, respectively, are

found to be composed of simple repeats. The most prominent simple repeat is the trinucleotide (TTG)<sub>n</sub> (in all six reading frames; see the ‘Methods’ section) that covered 19.1% and 18.5% of the CCMP1383 and CCMP2088 genome assemblies, respectively. The proportion of (TTG)<sub>n</sub>, observed as possible 3-mers of TTG, TGT, or GTT (each ~7–8%) in the assembled genomes, is very similar to that observed in the sequence read data (Fig. 1d and Additional file 3: Supplementary Table 6). Therefore, this observed prevalence of (TTG)<sub>n</sub> is unlikely due to assembly artefacts.

### DinoSL in full-length transcripts of *Polarella glacialis*

To generate high-quality supporting data to guide our gene-prediction workflow, we generated transcriptomes from both *P. glacialis* isolates, including full-length transcripts using PacBio IsoSeq technology (see the ‘Methods’ section). Mature nuclear transcripts of dinoflagellates are known to contain a 22-nucleotide *trans*-spliced leader sequence (DinoSL: DCCGTAGCCATTTGGCTCAAG, where D = T, A, or G) at the 5'-end [31]. Relic DinoSL sequences arise when transcripts with attached DinoSL are integrated back into the genome, expressed and *trans*-spliced with a new leader sequence [32]. Successive rounds of transcript re-integration result in multiple relic DinoSLs on a single transcript. We searched the full-length transcripts (435,032 in CCMP1383 and 1,266,042 in CCMP2088) for the presence of DinoSL and relic DinoSL sequences (see the ‘Methods’ section). DinoSL sequences were recovered in 13.54% and 50.39% of transcripts (hereinafter DinoSL-type transcripts) in CCMP1383 and CCMP2088, respectively (Additional file 3: Supplementary Table 7). An earlier study [33] reported a single transcript in CCMP2088 that has a non-canonical DinoSL sequence (ATCGTAGCCATGTTGGCTCAAG), but our exhaustive search against the transcripts in either isolate did not recover this sequence.

Although our experiment (see the ‘Methods’ section) was designed to recover full-length transcripts (with complete 5' and 3' regions), it is possible that the adopted library preparation step was suboptimal and the lack of a DinoSL in many transcripts may be explained by mRNA degradation. This may, in the first instance, be reflected by the varying degrees of truncation of the DinoSL-type transcripts in our data. However, 70.45% of these transcripts in CCMP1383 and 69.18% of transcripts in CCMP2088 start at one of the two contiguous cytosine bases (i.e. at positions 2 and 8) of the DinoSL (Fig. 2a and Additional file 3: Supplementary Table 8). This preference for start sites at the double-cytosine positions suggests that the 5' selection method we used (that purifies for the 5' methylated cap site) is binding to these regions instead of the true 5'-cap. This in turn may happen because cytosines at these sites are

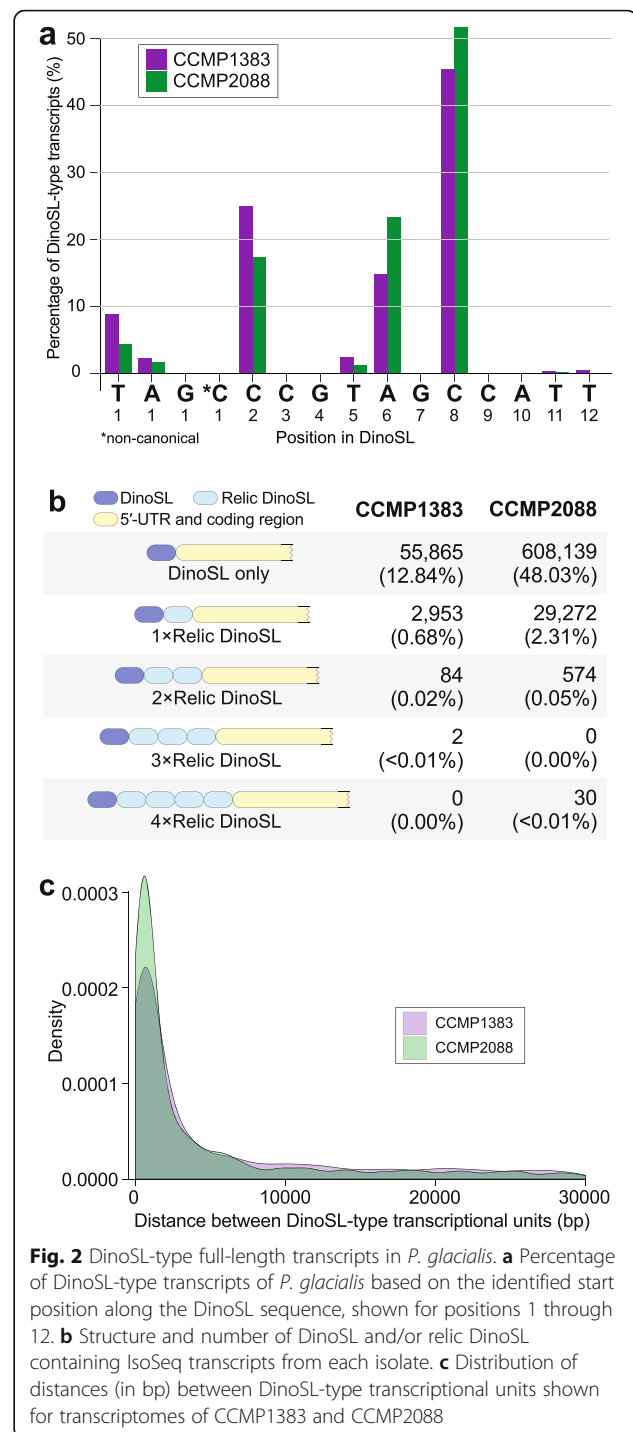


**Fig. 2** DinoSL-type full-length transcripts in *P. glacialis*. **a** Percentage of DinoSL-type transcripts of *P. glacialis* based on the identified start position along the DinoSL sequence, shown for positions 1 through 12. **b** Structure and number of DinoSL and/or relic DinoSL containing IsoSeq transcripts from each isolate. **c** Distribution of distances (in bp) between DinoSL-type transcriptional units shown for transcriptomes of CCMP1383 and CCMP2088

methylated. Cytosine methylation has been described in genomes of eukaryotes including dinoflagellates, potentially as a mechanism for silencing of transposable elements and regulation of gene expression [34–36]. A recent study of the *Breviolum minutum* genome revealed that cytosine methylation often occurred at CG dinucleotides [37]. The impact of methylation on recovery of



splice leaders in dinoflagellates remains to be systematically investigated.

In CCMP1383 and CCMP2088, 0.68% and 2.31% of all full-length transcripts, respectively, were found to encode one relic DinoSL (immediately following their primary DinoSL) while smaller proportions (0.020% and 0.048%, respectively) encode multiple relic DinoSL sequences (Fig. 2b). We recovered 30 transcripts in CCMP2088 that have four putative relic DinoSL sequences; they shared > 99% sequence identity among one another. Five of these 30 transcripts are shorter than the others, suggesting an alternative transcription 3'-termination site, thus a distinct isoform.

We further assessed the diversity of alternative splice forms by clustering the full-length transcripts by sequence similarity using PASA (see the 'Methods' section). Each resulting PASA 'assembly' [38] represents a distinct alternative isoform, and overlapping 'assemblies' constitute a transcriptional unit (Additional file 3: Supplementary Table 9). We identified 30,463 and 22,531 alternative isoforms comprising 24,947 and 19,750 transcriptional units in CCMP1383 and CCMP2088, respectively. When focusing only on DinoSL-type transcripts, these numbers are 8714 and 6576, comprising 7146 and 5110 transcriptional units, respectively (Additional file 3: Supplementary Table 9). In both isolates, alternative exons are the most common events observed among all transcript isoforms (e.g. 45.85% of all inferred events in CCMP2088), followed by alternative donor (22.05%) and acceptor (20.43%) sites (Additional file 3: Supplementary Table 10).

The addition of DinoSL sequences was proposed to be a mechanism to split polycistronic pre-mRNA into monocistronic mature mRNA [31]. A little over one half (50.45% in CCMP1383, 58.78% in CCMP2088) of these DinoSL-type transcriptional units are located within 5 Kbp of one another (Fig. 2c). Interestingly, among the DinoSL-type transcript isoforms, the two most enriched Pfam domains in both isolates are bacteriorhodopsin-like protein (PF01036) and cold-shock DNA-binding (PF00313) (Additional file 3: Supplementary Table 11). To further assess the functional diversity of DinoSL-type transcripts, we sequenced 747,959 full-length transcripts from CCMP1383 specifically selected for DinoSL (see the 'Methods' section and Additional file 3: Supplementary Table 7). These transcripts comprised only 1187 isoforms (3.9% of the total 30,463 isoforms; see Additional file 3: Supplementary Table 9). Similar functions are prevalent among these genes (Additional file 3: Supplementary Table 11), thus lending support to our observation of functional bias in DinoSL-type transcripts. In addition, the frequency at which DinoSL-type transcripts are integrated back into the genome is likely dependent on their relative abundance in the nucleus. Therefore, transcripts containing relic DinoSLs are likely

to be, or have been, highly expressed. In both isolates, the ice-binding (DUF3494) and the bacteriorhodopsin-like protein domains, both important for adaptation to cold (see below), are among the most enriched features in transcripts encoded with a relic DinoSL.

#### Prediction of protein-coding genes in *Polarella glacialis* is likely impacted by RNA editing

Using a gene-prediction workflow customised for dinoflagellate genomes [39] (see the 'Methods' section), we predicted 58,232 and 51,713 protein-coding genes (hereinafter *genes*) in the CCMP1383 and CCMP2088 genomes, respectively (Table 2 and Additional file 3: Supplementary Table 12). Of the 58,232 genes predicted in CCMP1383, 51,640 (88.68%) of the encoded proteins were recovered in CCMP2088 (Fig. 3a). Likewise, of the 51,713 genes predicted in CCMP2088, 46,228 (89.39%) of the encoded proteins were recovered in CCMP1383 (Fig. 3a). The difference in the numbers of predicted genes and sequence dissimilarity observed between the two genomes could be explained in part by the presence of distinct transcript isoforms. Although transcriptome evidence can improve the quality of predicted genes, our results indicate that this evidence can also complicate prediction when a gene has multiple isoforms, more so when these isoforms are recovered unevenly between the two isolates. The generation of alternatively spliced mRNAs is likely explained by local adaptation in the polar regions that drives functional diversification.

Interestingly, almost all predicted proteins not recovered in the proteins of the counterpart isolate (i.e. 6003 of 6592 in CCMP1383 and 4660 of 5485 in CCMP2088) were recovered in the transcriptome of the counterpart isolate (Fig. 3a). These results indicate that some transcriptome evidence was not incorporated in ~10% of the predicted genes in each genome. We hypothesise that this is likely due to RNA editing in *P. glacialis* (Fig. 3b). Post-transcriptional editing of mRNAs is known to implicate nuclear-encoded genes of *Symbiodinium microadriaticum* [40] and organellar genes of other dinoflagellates [41–43]. RNA editing may introduce changes in the transcripts (e.g. base substitutions or indels) affecting the identification of open reading frames (e.g. disruption by in-frame stop codons or correction of premature stop codons) in the genome sequences, and thus impacting prediction of gene models. DNA modification in the form of methylation, although known in dinoflagellate genomes to affect gene expression [25, 35] and transposon silencing [37], does not appear to impact the technical process of genome and transcriptome sequencing [11–15]. Based on our data, we cannot dismiss the impact of these modifications on RNA editing and post-transcriptional modifications.

**Table 2** Predicted gene models in *P. glacialis* compared to representative publicly available dinoflagellate genomes. A more-comprehensive summary including gene models from all available dinoflagellate genomes is shown in Additional file 3: Supplementary Table 12. Genes from the Symbiodiniaceae taxa are based on the revised predictions from Chen et al. [39]

	<i>Polarella glacialis</i>		Symbiodiniaceae				Parasitic
	CCMP1383	CCMP2088	<i>Symbiodinium microadriaticum</i>	<i>Breviolum minutum</i>	<i>Cladocopium goreau</i>	<i>Fugacium kawagutii</i>	<i>Amoebophrya ceratii</i>
<b>Genes</b>							
Number of genes	58,232	51,713	29,728	32,803	39,006	31,520	19,925
Gene models supported by transcriptome (%)	94.0	94.3	79.2	89.4	76.5	69.0	24.4
G+C content of CDS (%)	57.84	57.78	57.43	51.18	54.23	54.19	60.77
<b>Exons</b>							
Number of exons per gene	11.64	10.84	19.21	19.03	12.46	11.63	3.39
Average length (bp)	105.67	108.71	115.44	101.38	130.47	158.13	577.84
Total length (Mb)	71.60	60.94	65.92	63.30	63.42	57.96	39.08
<b>Introns</b>							
Number of genes with introns (%)	73.79	75.60	95.70	93.74	96.00	96.00	71.35
Average length (bp)	1408	1296	387.92	451.33	593.53	658.41	337.11
Total length (Mb)	837.95	636.20	210.00	267.00	265.35	220.58	16.08
<b>Intergenic regions</b>							
Average length (bp)	21,625	20,922	15,108	5983	9538	18,050	1525

*Hematodinium* sp. is not shown as no predicted genes were reported

Given the diploid genome assembly for each isolate, we assume that the number of predicted genes would be approximately twice the number expected in a haploid genome (e.g. 50,000 genes in a diploid assembly versus 25,000 in a haploid assembly); this number remains a rough estimate, because the delineation of a haploid *P. glacialis* genome remains to be systematically investigated with genome data at chromosomal resolution. The workflow used to predict genes in the Symbiodiniaceae genomes is the same as used in this study [39], making the predicted gene features more comparable. As expected, the number of predicted genes in all six (haploid) genomes of Symbiodiniaceae is roughly similar to the rough estimate of haploid gene number for the two *P. glacialis* genomes (Table 2 and Additional file 3: Supplementary Table 12). The proportion of genes predicted in *P. glacialis* that are supported by transcriptome evidence (~94% for each isolate; Table 2) is much higher than in the Symbiodiniaceae isolates (~79% averaged among six genomes [39]). This result may be explained by the more extensive transcriptome data we generated in this study (using both RNA-Seq short-read and Iso-Seq full-length transcripts) to guide our gene prediction workflow (see the 'Methods' section), compared to the transcriptome data (based on RNA-Seq short-reads) available for the other isolates.

Sequences of tRNAs and rRNAs appear to be abundant in both genome assemblies (Additional file 3:

Supplementary Table 13; see the 'Methods' section); 9485 tRNAs were predicted in CCMP1383 and 9268 in CCMP2088. These sequences have not been systematically investigated in dinoflagellate genomes and are much more abundant than the 329 reported in the genome of the green alga *Chlamydomonas reinhardtii* [44]. However, this result is not unexpected because repetitive elements are known to give rise to tRNA pseudogenes [45], and repetitive elements are abundant in the *P. glacialis* genomes. Likewise, we predicted 297 and 3021 rRNA sequences in CCMP1383 and CCMP2088, respectively. This observation is caused by the differential abundance of 5S rRNAs (255 in CCMP1383 versus 2983 in CCMP2088) predicted in the genome assemblies; 5S rRNAs are known to be highly duplicated in eukaryote genomes [46]. Given that both genome assemblies remain fragmentary, and about 68% of genomic regions is repetitive, functional validity and structural integrity of these tRNAs and rRNAs in *P. glacialis* remain to be systematically investigated using a chromosomal-level genome assembly.

#### Unidirectional tandem single-exon genes in *P. glacialis*

In *P. glacialis*, the longer intergenic regions are largely comprised of repeats (Additional file 2: Supplementary Fig. 3). Roughly one third of the intergenic regions (35.86% in CCMP1383; 34.97% in CCMP2088) are ≤ 5 Kbp in length. The fraction of these regions covered by repetitive elements is 32.92% (CCMP1383) and

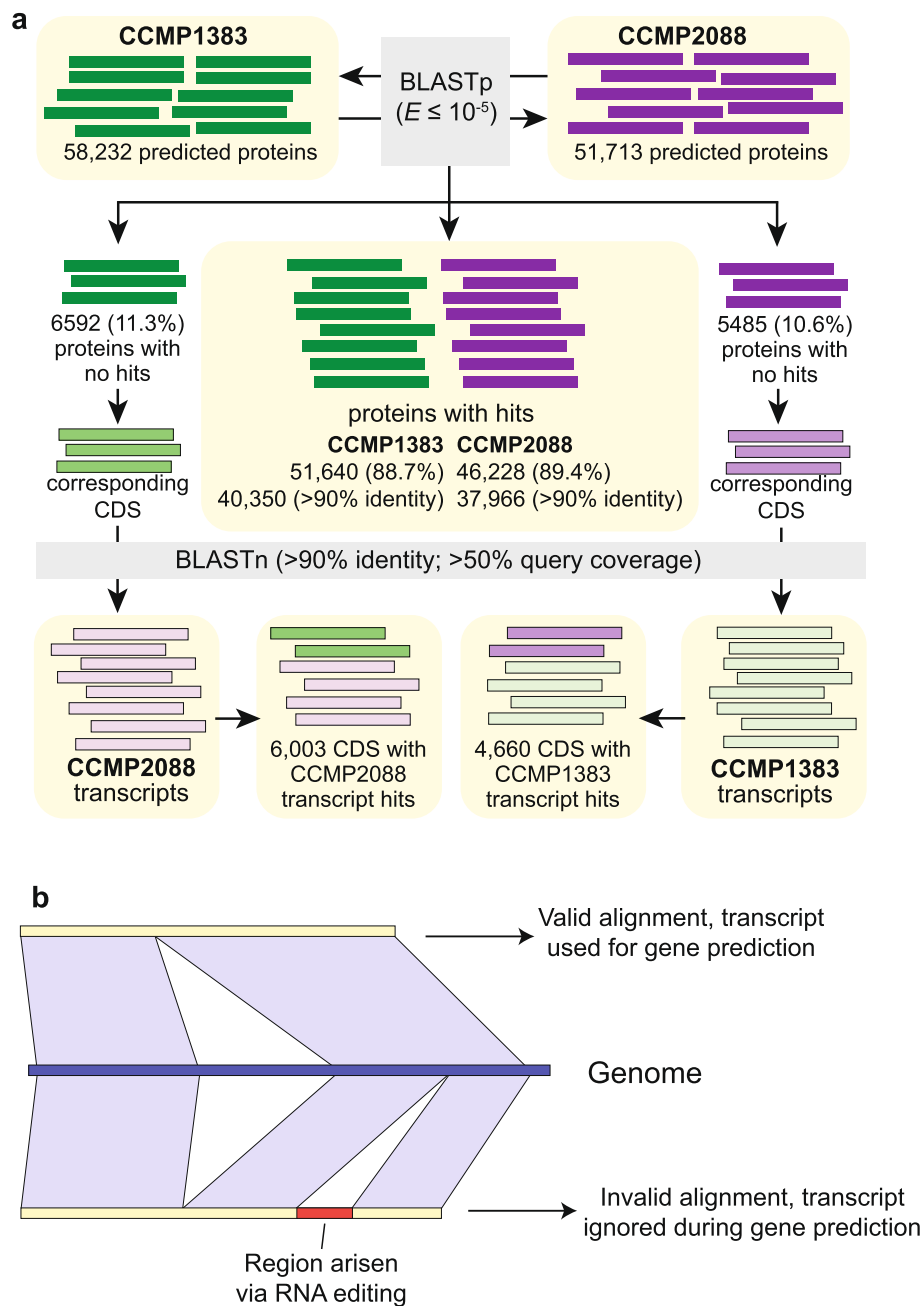
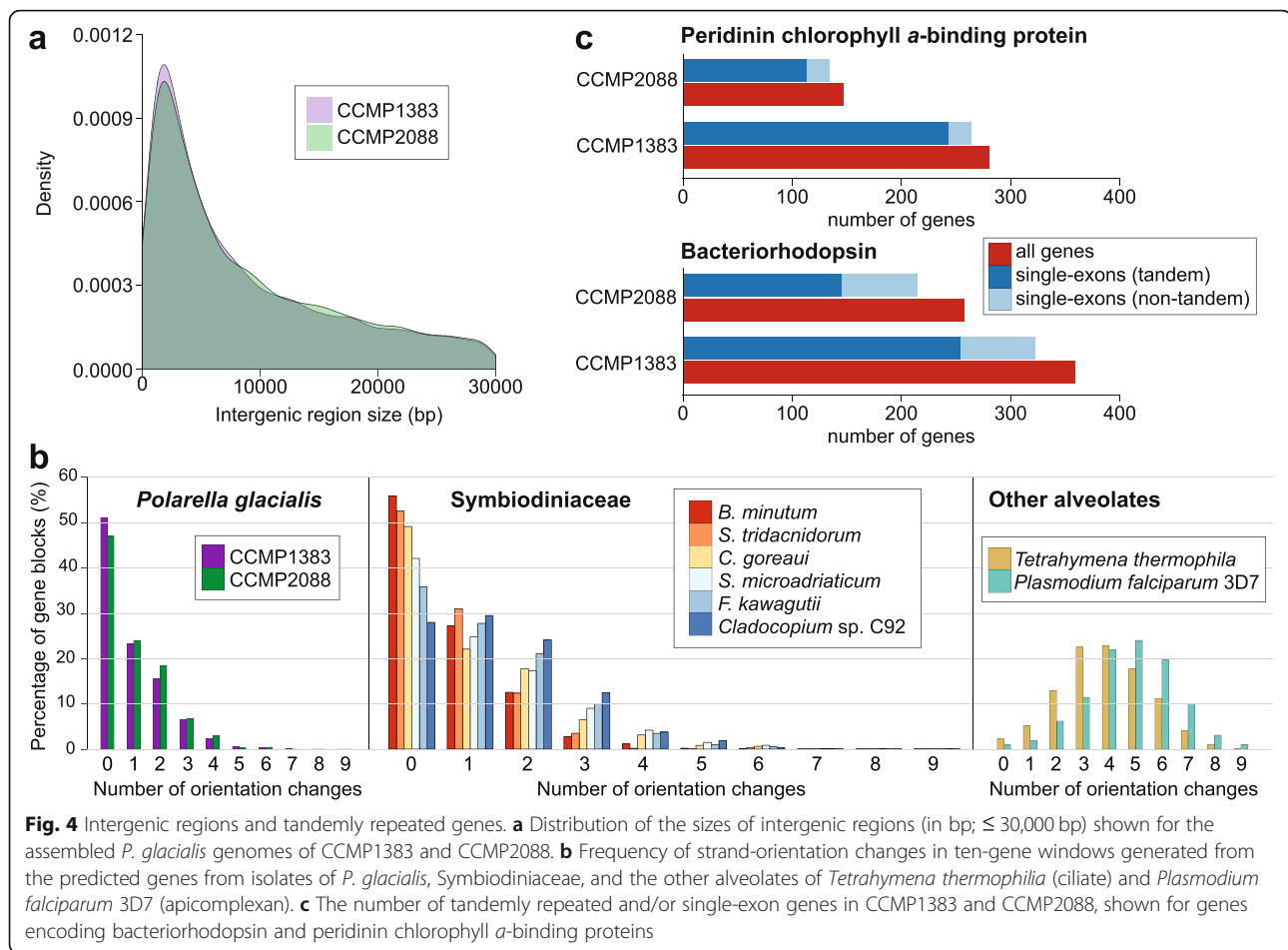


**Fig. 3** Comparison of predicted gene models between the two *P. glacialis* genomes. **a** The comparison of predicted proteins in CCMP1383 against those in CCMP2088 is shown, incorporating evidence from the corresponding transcriptome data. **b** Scenario of RNA editing that would disrupt the alignment of a transcript to the genome

32.93% (CCMP2088; see Additional file 2: Supplementary Fig. 3); these numbers are 59.65% and 59.05% (see Additional file 2: Supplementary Fig. 3) among intergenic regions > 5 Kbp. This observation suggests that the expansion of repeats is greater in, and likely contributes to, longer intergenic regions in the genome. Based on the lengths of intergenic regions, we assessed the tendency of protein-coding genes to be located in close

proximity to one another. We define a gene cluster as two or more genes that are separated by intergenic regions  $\leq 5$  Kbp in length. Approximately 50% of the analysed genes (26,580 in CCMP1383; 21,376 in CCMP2088) appear to satisfy this criterion (Fig. 4a), indicating a tendency for these genes to occur in clusters (10,405 clusters in CCMP1383 and 8608 in CCMP2088). Adjacent genes were clustered if their intergenic regions





were  $< 5$  Kbp, and clusters were considered unidirectional if all genes in that cluster were encoded in the same direction. Remarkably, almost all of these clustered genes (24,276 and 19,544 respectively for those of CCMP1383 and CCMP2088;  $\sim 40\%$  of total genes in each genome) are encoded unidirectionally. These unidirectional gene clusters (9572 in CCMP1383 and 7922 in CCMP2088) may represent a mechanism in *P. glacialis* (and potentially the order Suessiales) to ensure transcriptional efficiency, with genes in close physical proximity potentially transcribed together. In some cases, these gene clusters encode the same or similar functions; for example, 22 unidirectionally encoded genes in CCMP1383 (and 19 in CCMP2088) putatively encode the major basic nuclear protein 2.

The small number of strand-orientation changes within ten-gene windows was used in the genome study of *B. minutum* [14] to illustrate the tendency for genes to be encoded unidirectionally. Using the same approach, *P. glacialis* and other Symbiodiniaceae taxa were found to encode genes unidirectionally, with most ten-gene windows having no more than three strand-orientation changes (Fig. 4b). In contrast, this pattern

was not observed in the genomes of other alveolates (i.e. the ciliate *Tetrahymena thermophila* and the apicomplexan *Plasmodium falciparum* 3D7), for which most ten-gene windows have three to six strand orientation changes (Fig. 4b). Whereas this analysis does not consider the distance between genes, the unidirectionality of coding regions reflects a feature common within the order Suessiales (and potentially all dinoflagellates).

Among the predicted genes in both genomes, 4898 (CCMP1383; 8.4%) and 3359 (CCMP2088; 6.5%) are located (nested) within introns of multi-exon genes. Although most cases (71.02% in CCMP1383 and 74.90% in CCMP2088) represent one nested gene per multi-exon gene, in extreme cases, we observed 18 (CCMP1383) and 24 (CCMP2088). Additional file 2: Supplementary Fig. 4 shows an example of 15 nested genes of CCMP1383 spanning three introns of the gene putatively encoding an alanine-tRNA ligase. Among the nested genes within each intron, five encode fucoxanthin chlorophyll *a/c*-binding protein, and four, light-harvesting complex protein. The validity of the nested gene structure was confirmed by the expression evidence based on full-length transcripts.

Of particular interest, we recovered 15,263 (26.2%) and 12,619 (24.4%) single-exon genes in CCMP1383 and CCMP2088, respectively (Table 2). These proportions are higher than those in symbiodiniacean genomes (< 12% of genes; Table 2 and Additional file 3: Supplementary Table 12). Of all recovered single-exon genes, > 80% are found in both isolates, and almost all (99.08% of those in CCMP1383, 98.12% of those in CCMP2088) are supported by transcriptome evidence (including full-length transcripts that were selected for 5'-cap and 3'-polyadenylation sites). These results suggest that these genes are bona fide *P. glacialis* genes (i.e. not bacterial contaminants, nor artefacts of our gene prediction workflow). Many of the Pfam domains enriched in the single-exon genes are also enriched in the predicted genes of *P. glacialis* compared with symbiodiniacean genes (see also below and Additional file 3: Supplementary Table 14). Enriched features of *P. glacialis* such as bacteriorhodopsin-like protein (PF01036), peridinin-chlorophyll *a*-binding (PF02429), and DUF3494 (PF11999) are encoded as single-exon genes. A number of other domains are enriched in the single-exon genes in both *P. glacialis* isolates. The bacterial DNA-binding protein domain (PF00216), which is predominantly found in bacteria, is enriched and potentially has arisen in *P. glacialis* via lateral genetic transfer. The reverse transcriptase (PF00078) domain is also enriched and is likely involved in the activity of retrotransposons in the *P. glacialis* genomes.

#### What makes *Polarella Polarella*?

We compared the annotated functions of *P. glacialis* genes against those from other Symbiodiniaceae genomes [12–15]. When comparing the annotated Pfam domains, we observed a significant over-representation of DUF3494 (PF11999), cold-shock (PF00313), and chlorophyll *a*-binding (PF00504) domains in *P. glacialis* relative to Symbiodiniaceae (Additional file 3: Supplementary Table 15), as we previously observed in an independent transcriptome analysis [47]. In this study using high-quality gene models predicted from genome data, we also observed over-representation (adjusted *p* value  $\leq 10^{-40}$ ) of pentatricopeptide repeat (PF13041, PF13812, PF01535), ATP synthase subunit C (PF00137), bacteriorhodopsin-like protein (PF01036), and peridinin-chlorophyll *a*-binding (PF02429) in *P. glacialis*. Having genes that encode important functions arranged as tandem repeats may provide *P. glacialis* a mechanism to quickly increase their expression or to maintain or regulate high expression of these genes. Among the tandemly repeated genes (see the 'Methods' section), the over-represented domains include those related to energy production, e.g. RuBisCO (PF00016 and PF02788) and carbonic anhydrase (PF00484); metabolism, e.g. glyceraldehyde 3-phosphate dehydrogenase (PF00044 and PF02800) involved in glycolysis; and the ribosomal

complex (e.g. PF00252, PF01283, and PF01655); see Additional file 3: Supplementary Table 16 for details. Interestingly, the peridinin-chlorophyll *a*-binding and bacteriorhodopsin-like domains are predominantly encoded in blocks of tandemly repeated single-exon genes, implicating hundreds of genes in *P. glacialis* (Fig. 4c). All but one of these gene blocks (i.e. a contiguous region containing two or more genes) are unidirectionally encoded. Within each isolate, some of these features (e.g. peridinin-chlorophyll *a*-binding and bacteriorhodopsin-like domains) were also enriched among the tandemly repeated genes in *P. glacialis* (when compared against all genes within each *P. glacialis* isolate; see Additional file 3: Supplementary Table 16). Peridinin-chlorophyll *a*-binding protein (PCP) was thought to be encoded as 5000 single-exon gene copies in tandem repeat blocks in the bloom-forming dinoflagellate *Lingulodinium* (= *Gonyaulax*) *polyedra* [21], and these coding genes are thought to be monocistronic [48]. This protein may be universally important in free-living dinoflagellates, and potentially to a lesser extent among symbiotic lineages of these algae [49]. The tendency of tandemly repeated genes to have fewer introns was also reported in the bloom-forming *Amphidinium carterae* [50]. In combination with our other results (above), our observations suggest gene family expansion through tandem duplication drives the genome evolution of *P. glacialis*, and potentially of other free-living dinoflagellates. The use of a DinoSL sequence to split polycistronic transcripts into mature RNAs [31] may facilitate this mechanism.

Bacterial-derived rhodopsin, a transmembrane protein involved in bacterial phototrophy independent of chlorophyll through retinal binding, is encoded in diverse dinoflagellate lineages [51, 52]. The proton-pump type rhodopsins can create a proton gradient to drive synthesis of ATPase, in lieu of photosynthesis [53, 54]. An earlier gene expression analysis of the bloom-forming *Prorocentrum donghaiense* [55] revealed that proton-pump rhodopsins may compensate for photosynthesis under light-deprived conditions. These rhodopsins were also found to be highly expressed in diatoms under iron-deficient conditions [56]. All genes in both *P. glacialis* isolates have top hits to the sequences encoding proton-pump rhodopsins in *Oxyrrhis marina*. These rhodopsins were previously found to be more abundantly expressed in *O. marina* than the sensory-type rhodopsins involved in light harvesting for photosynthesis [57]. We hypothesise that the over-representation of rhodopsin and other photosynthesis-related genes in *P. glacialis* is an adaptation to light-limited (and potentially iron-limited) conditions, as expected in the ice brine channels where one of the samples was collected [10].

For each tandemly repeated PCP gene block, the coding and intergenic regions are highly conserved, on average sharing ~98% and ~95% sequence identity, respectively,

among all implicated blocks for both *P. glacialis* isolates (Additional file 3: Supplementary Table 17). These numbers compare to ~98% identity among coding regions, and ~89% among intergenic regions for each bacteriorhodopsin gene block. This result suggests that these tandemly repeated genes are a recent innovation in the *P. glacialis* genome, or more likely, that these genes are highly conserved under strong selective pressure. Both homodimeric and monomeric forms of PCPs have been described in dinoflagellates [21, 58]; the conserved intergenic (spacer) regions in the tandem PCP gene blocks were previously proposed as species-specific PCP transcriptional promoters [21, 49] in dinoflagellates, although this hypothesis remains to be experimentally validated.

A previous study based on transcriptome analysis [47] revealed ‘dark’ proteins (i.e. they lack an annotation based on standard sequence similarity searches against characterised proteins; see the ‘Methods’ section) that are conserved and/or lineage-specific in dinoflagellates. Using 302,231 protein sequences predicted from the genome data of *P. glacialis* and six Symbiodiniaceae species (see Additional file 3: Supplementary Table 18), we constructed 35,751 putatively homologous protein sets that consist of 85.3% of the total protein sequences analysed. Of these sets, 8673 (24.26%) containing 10.63% of the clustered proteins (27,425 proteins; 9.07% of 302,231) were classified as dark. The number of dark proteins (and hence dark genes) from each dataset (see Additional file 3: Supplementary Table 18) was largely congruent with the proportions of dark genes reported previously [47]. Of the 8673 dark homologous sets, 4602 (53.06%) contain sequences from only *P. glacialis*; 4540 (98.65% of the 4602) contain sequences from both isolates, so they are unlikely to have arisen due to assembly artefacts. We consider a dark set as single-exonic if all its members are encoded in single exons, and a dark set as multi-exonic if at least one member is encoded in multiple exons. Following this definition, most (3149; 68.43%) of the 4602 *P. glacialis*-specific sets are multi-exonic, whereas 1453 (31.57%) are single-exonic. Of the 1453 single-exonic dark sets, 714 (49.14%) are supported by IsoSeq data and 1449 (99.72%) by IsoSeq and/or RNA-Seq data. Therefore, these genes likely represent true genetic (and functional) innovations specific to *P. glacialis*.

#### Single evolutionary origin of ice-binding domains in dinoflagellates

The Pfam domain DUF3494, a known ice-binding domain [59], is over-represented in cold-adapted dinoflagellates [47]. In both *P. glacialis* isolates (see Additional file 3: Supplementary Table 19), most putative ice-binding genes encode only the DUF3494 domain. They are encoded in single exons and in unidirectional, tandemly repeated

blocks, potentially as a mechanism to enhance the efficiency of gene expression. Interestingly, the intergenic regions within each tandem gene block are more conserved (mean > 94% identity) and less variable (standard deviation ~3% for both species) than the coding regions (mean ~92% identity; Additional file 3: Supplementary Table 17). The conserved intergenic (spacer) regions lend support to the notion that these regions may serve as transcriptional promoters, as has been postulated for the PCP genes [21, 49]. Because the DUF3494 domain in many species has arisen via lateral genetic transfer [59], the presence of these genes in this configuration suggests that they might have arisen via the same mechanism in *P. glacialis*.

Figure 5 shows part of a phylogenetic tree reconstructed with 1080 sequences of available DUF3494 domains encompassing Archaea, Bacteria, and eukaryotes; the complete tree is available as Additional file 4: Supplementary Data 1. All DUF3493 sequences from the dinoflagellates (*P. glacialis*, *Heterocapsa arctica*, *Scrippsiella hangoei*, and *Peridinium aciculiferum*), plus some sequences from the ice diatom *Fragilariopsis cylindrus*, form a strongly supported clade (bootstrap support [BS] = 100% based on ultrafast bootstrap approximation [60]) (Fig. 5). Within this dinoflagellate + diatom clade, the 169 DUF3494 sequences from *P. glacialis* (97 from CCMP1383, 72 from CCMP2088) form a strongly supported monophyletic clade (BS 100%), indicating that these domains in *P. glacialis* have an evolutionary history that is distinct from other dinoflagellates. In comparison, the domains in the ice diatom *F. cylindrus* were recovered in three distinct clades on the tree (two shown in Fig. 5), indicating their independent origins. As previously reported, DUF3494 domains in eukaryotes trace their origins to multiple events of lateral genetic transfer from bacteria and other eukaryotes [61, 62]. We also observed this pattern in our phylogenetic analysis although the origin of these domains in dinoflagellates remains unclear, with potential sources being Proteobacteria, Bacteroidetes/Chlorobi, or Euryarchaeota that also gave rise to the domains in some fungal species. Fungi are also distributed in multiple clades on this tree (see Additional file 4: Supplementary Data 1). The DUF3494 domains we recovered from the bacterial genomes (see the ‘Methods’ section, Additional file 1: Supplementary Note [12, 63–65], and Additional file 2: Supplementary Fig. 5) were grouped with their closely related species within the corresponding phylum (i.e. Proteobacteria and Bacteroidetes/Chlorobi) in distinct clades, indicating that they are indeed prokaryotic. These results indicate that all ice-binding domains in dinoflagellates share a single common origin likely from a Proteobacteria or Bacteroidetes/Chlorobi source and that those specific to *P. glacialis* have a distinct evolutionary history that may reflect niche specialisation.

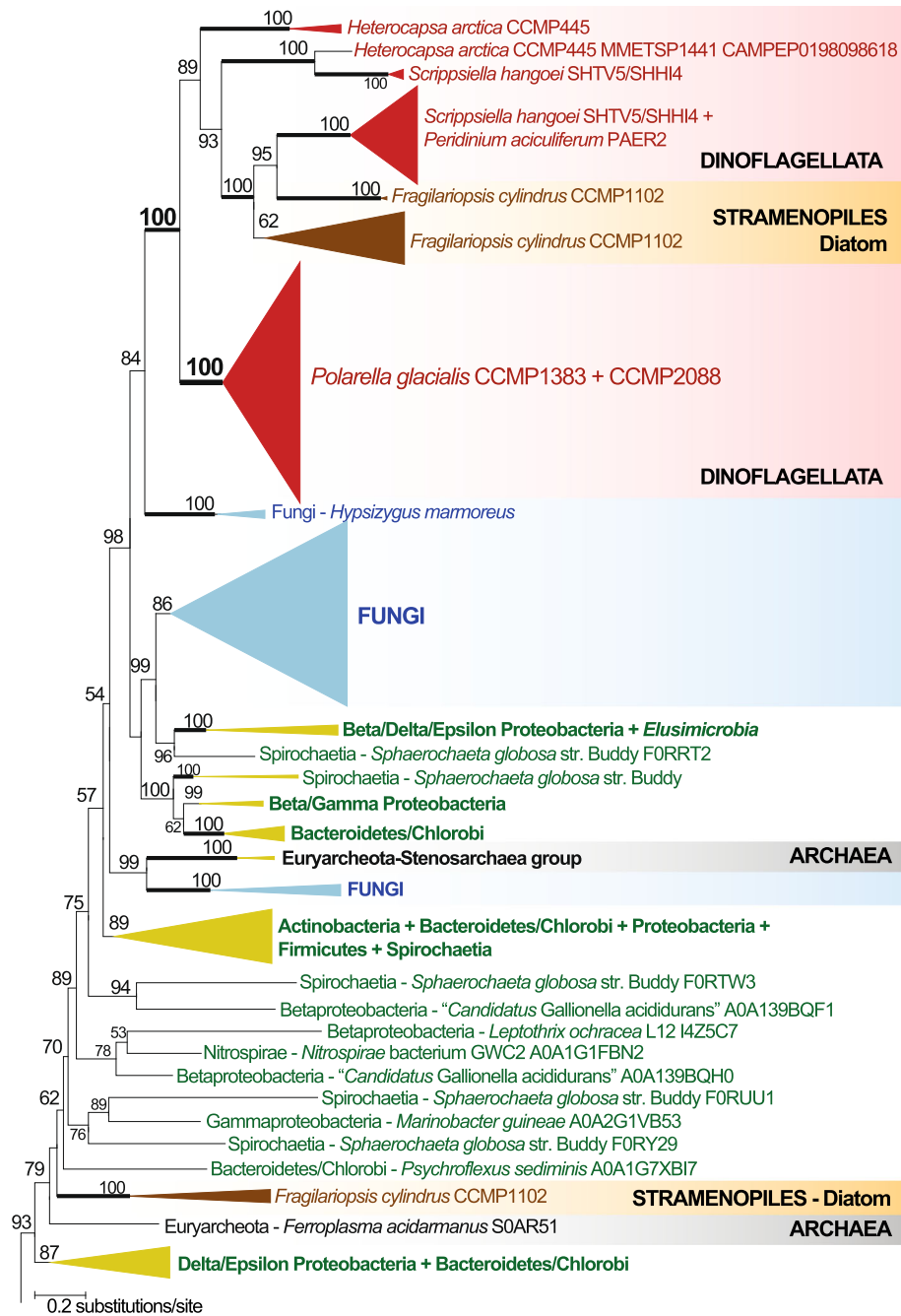


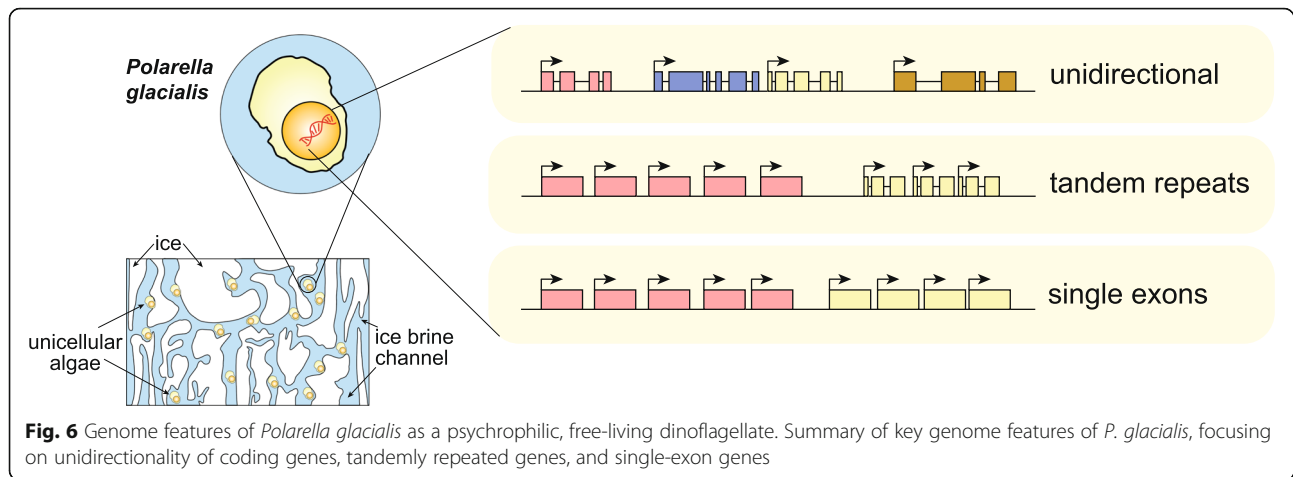
**Fig. 5** Evolutionary history of ice-binding domains in *P. glacialis* and dinoflagellates. Only a small part of the 1080-taxon maximum likelihood protein tree is shown. Support values, based on 2000 ultrafast bootstrap approximations, are shown at the internal nodes. Only values > 50% are shown. The unit of branch length is the number of substitutions per site

## Discussion

We generated two draft de novo diploid assemblies of *P. glacialis*, the first of any free-living psychrophilic dinoflagellates, and high-quality gene models supported by full-length transcriptomes. Genome features of *P. glacialis* (Fig. 6) elucidate how the genomes of dinoflagellates have evolved to adapt in a harsh environment. The

difference in genome sizes between the two isolates highlights the extensive structural divergence of genomes within a dinoflagellate species. The abundance of repetitive elements and LTRs in the genomes suggests their important role in shaping the genome evolution of these isolates, potentially contributing to the genome size difference. The molecular mechanisms and selective





pressure that contribute to the larger genome size in the Antarctic versus the Arctic isolate remain an open question and can best be addressed using assembled genomes at chromosomal resolution.

The *trans*-spliced DinoSL was thought to be a global signature of all transcripts in dinoflagellates, but our results reveal only a small proportion of full-length transcripts encode DinoSL (and with relic DinoSLs) and remarkably, these transcripts mostly encode functions that are critical for adaptation to cold and to low-light conditions, both relevant to the natural habitat of *P. glacialis* in ice brine channels. In addition, genes encoding these functions are unidirectionally encoded, often in a tandemly repeated single exonic structure. This distinctive gene organisation is likely a feature of free-living dinoflagellates, and may serve to enhance transcriptional efficiency of critical functions. The independently evolved ice-binding domains and the lineage-specific dark genes in *P. glacialis* highlight functional innovation in dinoflagellate genomes relevant to environmental adaptation and niche specialisation as successful psychrophiles in the extreme cold environment.

## Conclusions

Our results elucidate how selection acts within the context of a complex genome structure to facilitate local adaptation. Given the fact that most dinoflagellate genes show constitutive expression, *Polarella glacialis* has utilised a variety of strategies to enhance transcriptional response, including the tandem duplication in a unidirectional orientation of single-exon genes that encode functions critical to survival in cold, low-light polar environments. The data and knowledge generated from this study provide a foundational genomic reference for future research in dinoflagellate evolution, e.g. the evolutionary transition from free-living to symbiotic lifestyles, and the diversification of bloom-forming, toxin-producing species.

## Methods

### Cultures of *Polarella glacialis*

The cultures of *Polarella glacialis* isolates were acquired from the National Center for Marine Algae and Microbiota at the Bigelow Laboratory for Ocean Sciences, ME, USA. Both cultures were maintained in f/2 medium without silica [66] (100 mL culture in 250 mL conical flasks, 12-h:12-h light-dark cycle, 90  $\mu\text{mol photon m}^{-2} \text{s}^{-1}$ , 4 °C). The cultures were treated with ampicillin (100  $\mu\text{g mL}^{-1}$ ), kanamycin (50  $\mu\text{g mL}^{-1}$ ), and streptomycin (50  $\mu\text{g mL}^{-1}$ ) for 24 h before cell harvest. For extraction of nucleic acids, the cells (50 mL;  $> 10^6$  per mL) were harvested by centrifugation (3000g, 5 min). The resulting cell pellet was rinsed with 0.22- $\mu\text{m}$  filtered artificial seawater (Instant Ocean salt mixture, 33.3 g L<sup>-1</sup>; 1 mL), transferred to a 1.5-mL tube, and collected by further centrifugation (3000g, 5 min). The supernatant (seawater) was removed, and the tube was immediately snap-frozen with liquid nitrogen and stored at -80 °C until DNA/RNA extraction.

### Extraction of genomic DNA and total RNA

Genomic DNA was extracted following the 2xCTAB protocol with modifications. The cells were suspended in a lysis extraction buffer (400  $\mu\text{L}$ ; 100 mM Tris-Cl pH 8, 20 mM EDTA pH 8, 1.4 M NaCl), before silica beads were added. In a freeze-thaw cycle, the mixture was vortexed at high speed (2 min) and immediately snap-frozen in liquid nitrogen; the cycle was repeated 5 times. The final volume of the mixture was made up to 2% w/v CTAB (from 10% w/v CTAB stock; kept at 37 °C). The mixture was treated with RNase A (Invitrogen; final concentration 20  $\mu\text{g/mL}$ ) at 37 °C (30 min) and Proteinase K (final concentration 120  $\mu\text{g/mL}$ ) at 65 °C (2 h). The lysate was then subjected to standard extractions using equal volumes of phenol to chloroform to isoamyl alcohol (25:24:1 v/v; centrifugation at 14,000g, 5 min, RT) and chloroform to isoamyl alcohol (24:1 v/v;



centrifugation at 14,000g, 5 min, RT). DNA was precipitated using pre-chilled isopropanol (gentle inversions of the tube, centrifugation at 18,000g, 15 min, 4°C). The resulting pellet was washed with pre-chilled ethanol (70% v/v), before being stored in Tris-HCl (100 mM, pH 8) buffer. Total RNA was extracted using RNeasy Plant Mini Kit (Qiagen) following the manufacturer's protocol. The concentration of DNA or RNA was determined with NanoDrop (Thermo Scientific), and a sample with A230:260:280  $\approx$  1.0:2.0:1.0 was considered appropriate for sequencing.

#### Generation of genome data

For generation of short-read sequence data, samples of genomic DNA were sequenced using Illumina HiSeq2500 (Australian Genome Research Facility, Melbourne) and HiSeq4000 (Translational Research Institute and the Australian Genome Research Facility, Brisbane) platforms (see Additional file 3: Supplementary Table 20). For each isolate, two paired-end TruSeq libraries (inserts of  $\sim$ 250 bp and 600 bp for HiSeq2500;  $\sim$ 350 bp and  $\sim$ 600 bp for HiSeq4000) and three mate-pair Nextera libraries (inserts of  $\sim$ 2, 5, and 10 Kb) were generated for sequencing (in  $2 \times 150$  bases). In total, we generated 399.3 Gbp ( $\sim$ 132 $\times$  coverage based on the estimated diploid genome size) of Illumina short-read sequencing data for CCMP1383 and 746.7 Gbp ( $\sim$ 281 $\times$  coverage) for CCMP2088 (see Additional file 3: Supplementary Table 20).

For generation of long-read data, samples of genomic DNA were sequenced using the PacBio Sequel platform available at the Queensland University of Technology Central Analytical Research Facility and at the Ramaciotti Centre of Genomics (University of New South Wales, Sydney). DNA fragments of lengths 10–20 kb were selected for the preparation of sequencing libraries. In total, 15 SMRT cells were sequenced for CCMP1383 producing 9.3 million subreads (74.6 Gbp) and 7 SMRT cells for CCMP2088 generating 4 million subreads (35.9 Gbp), see Additional file 3: Supplementary Table 2 for details.

#### Generation of transcriptome data (RNA-Seq)

For generation of RNA-Seq data, total RNA samples were sequenced at the Australian Genome Research Facility (Brisbane) using the Illumina HiSeq4000 platform. Illumina paired-end ( $2 \times 150$  bp reads) RNA-Seq data was generated for both CCMP1383 (55.4 Gbp) and CCMP2088 (61.7 Gbp), see Additional file 3: Supplementary Table 21 for details.

#### Generation of full-length transcript data (PacBio IsoSeq)

Using the extracted total RNA samples (above), a full-length cDNA library was constructed for each of CCMP1383 and CCMP2088 using the TeloPrime Full-

Length cDNA Amplification Kit (Lexogen, Vienna) following the kit manual. Two cDNA synthesis reactions were carried out in parallel for each sample, with 2  $\mu$ g of total RNA used as a starting material in each reaction. Double-stranded cDNA resulting from the two reactions was combined before performing PCR amplification using the TeloPrime PCR Add-on Kit (Lexogen, Vienna). For each sample, 16 parallel PCRs were carried out using 22 amplification cycles and 2  $\mu$ L of double-stranded cDNA per reaction as a template; the PCR products were pooled together and then split into two fractions, which were purified using 1 $\times$  and 0.5 $\times$  AMPure PB beads (Pacific Biosciences, California), respectively, and pooled at equal molarity. For sample CCMP1383, a total of 2.52  $\mu$ g of purified full-length cDNA was obtained and was used for PacBio SMRTbell library preparation with the SMRTbell Template Prep Kit 1.0 (Pacific Biosciences, California); the library was sequenced on 4 SMRT cells v2 LR using 20-h movies on a Sequel platform at the Institute for Molecular Bioscience Sequencing Facility (University of Queensland, Brisbane). For CCMP2088, 1.95 ng of cDNA were obtained and submitted to the Ramaciotti Centre for Genomics (University of New South Wales, Sydney) for SMRTbell library preparation and sequencing on a PacBio Sequel System, also using 4 SMRT Cells v2 LR and 20-h movies.

In addition to the cDNA libraries described above, a spliced leader-specific transcript library was generated for CCMP1383. Four parallel PCR reactions were performed with the TeloPrime PCR Add-on Kit (Lexogen, Vienna) using 12 amplification cycles, conserved spliced leader fragment (5'-CCGTAGCCATTTTGGCTCAAG-3') as a forward primer, TeloPrime PCR 3' primer as a reverse primer, and 2  $\mu$ L of double-stranded cDNA synthesised using the TeloPrime Full-Length cDNA Amplification Kit (Lexogen, Vienna) as a template. The PCR products were pooled and purified (same method as above), resulting in 987 ng of cDNA. SMRTbell library construction was carried out using the PacBio SMRTbell Template Prep Kit 1.0, followed by sequencing on 2 SMRT cells v2 LR using 20-h movies on the Sequel at the Institute for Molecular Bioscience Sequencing Facility (University of Queensland, Brisbane). Data yield from each SMRT cell is detailed in Additional file 3: Supplementary Table 22. All genome and transcriptome sequencing data are available at NCBI GenBank via BioProject accession PRJEB33539.

#### Processing of sequence data

Adaptor sequences were removed, and low-quality bases trimmed from paired-end reads using Trimmomatic v0.35 (LEADING:10 TRAILING:10 SLIDINGWINDOW:4:30 MINLEN:50) [67] and overlapping read pairs (250 bp insert size) were merged using FLASH v1.2.11 (max-overlap 85) [68]. Mate-pair reads were processed using

the NextClip v1.3 pipeline [69] using the preliminary CLC assembly as a reference. Only the category A, B, and C mate-pair reads were retained from the NextClip analysis. Further trimming of the mate-pair reads to remove low-quality regions and adapters was performed using Trimmomatic v0.35 (LEADING:10 TRAILING:10 SLIDINGWINDOW:4:20 MINLEN:25).

Trimmed paired-end reads were mapped using bowtie2 [70] against the initial CLC assembly, and the mean insert size and standard deviation were computed using Picard tools v2.6.0 'CollectInsertSizeMetrics'. Mate-pair sequences were aligned only against scaffolds from the initial assembly with a length > 15 Kbp using bbmap (rcs = f pairedonly = t ambig = toss). The different approach taken for the mate-pair reads was to discard ambiguously mapped reads (i.e. reads that map equally well to multiple locations), because these reads complicate the estimation of insert size. The maximum insert size set during the alignment stage of both mate-pair and paired-end libraries was double the maximum expected insert size.

Illumina RNA-Seq data was trimmed for adapters and low-quality regions using Trimmomatic v0.35 (LEADING:10 TRAILING:10 SLIDINGWINDOW:4:30 MINLEN:50). PacBio IsoSeq data from each SMRT cell was polished (--polish) using the circular consensus sequencing tool (ccs v3.1.0 <https://github.com/PacificBiosciences/unanimity/blob/develop/doc/PBCCS.md>); only polished reads with a quality > 0.99 were retained. Primers were removed from the polished reads using lima v1.8.0 (<https://github.com/pacificbiosciences/barcoding>) in IsoSeq mode. Only reads with the correct 5-prime/3-prime primer configuration were retained. The PacBio IsoSeq tool v3.1.0 was used to remove concatemers (using the refine option) from the primer trimmed reads ([https://github.com/PacificBiosciences/IsoSeq3/blob/master/README\\_v3.1.md](https://github.com/PacificBiosciences/IsoSeq3/blob/master/README_v3.1.md)).

#### Genome size estimation using *k*-mers

The *k*-mer frequency distribution in the trimmed paired-end reads (including merged) was used to estimate genome size and to assess ploidy. Genome size estimation was conducted following the approach described in Liu et al. [12]. The enumeration of *k*-mers was performed using Jellyfish [71] at *k* = 17, 19, 21, 23, 25, 27, 29, and 31. The range of *k* used for the purpose of genome size estimation follows previously published studies of dinoflagellate genomes [11, 12]. For diploid genomes, a bimodal *k*-mer count distribution is expected, genome size estimated from the first peak represents the diploid state, and that estimated from the second peak represents the haploid state. The standard theoretical model of a diploid genome in GenomeScope [72] was used (*k*-mer size 21) to verify the diploidy observed in the sequence data (see Additional file 2: Supplementary Fig. 1).

#### De novo genome assemblies

Initial de novo assemblies for CCMP1383 and CCMP2088 were generated independently using CLC Genomics Workbench (v7.5) (default parameters; hereinafter CLC assemblies), incorporating all trimmed paired-end reads (using merged reads where applicable). The initial CLC assemblies were further processed using the Redundans package (retrieved 10 March 2019) [73] using the trimmed paired-end and mate-pair reads.

Final genome assemblies for each isolate were generated with MaSuRCA v3.2.8 [74] using untrimmed paired-end reads, trimmed mate-pair reads, and PacBio reads (> 5 Kbp). For each isolate, the parameters of estimated assembly size in MaSuRCA was set based on the average estimated haploid genome size (see Additional file 3: Supplementary Table 4); ploidy was set to two. Scaffolds < 1 Kbp were discarded from the final assembly. The MaSuRCA assembler will attempt to remove redundant and (when ploidy set to two) homologous scaffolds, producing a haploid assembly. For both isolates, this step was ineffective in identifying and collapsing homologous scaffolds into a haploid assembly.

Trimmed and merged paired-end reads were mapped using bowtie2 [70] against the corresponding MaSuRCA diploid assembly, and the purge\_haplotigs [75] program (v1.0.2; 'purge\_haplotigs contigcov -l 5 -m 63 -h 120' for CCMP1383 and 'purge\_haplotigs contigcov -l 40 -m 102 -h 170' for CCMP2088) was run in an attempt to reconstruct a haploid assembly for each isolate. Unfortunately, purge\_haplotigs was unable to fully reduce the CCMP1383 and CCMP2088 assemblies into haploid representations. As no reliable haploid assembly could be generated, the diploid assemblies generated by MaSuRCA were used for downstream analysis.

#### Identification and removal of archaeal, bacterial, and viral sequences

Identification and removal of contaminant sequences in the genome assemblies were assessed using a method similar to that of Aranda et al. [13]. Genome scaffolds were compared using BLASTN against a database of archaeal, bacterial, and viral genome sequences retrieved from RefSeq (release 88). Scaffolds were retained and considered non-contaminant, if  $\leq 10\%$  of their length was covered by BLAST hits with a bit score > 1000 and  $E \leq 10^{-20}$ . Further identification and removal of contaminant sequences were conducted following Chen et al. [39]. Scaffolds were removed if they had a G+C content and length outside the expected normal distribution; no putative contaminant scaffolds were identified using this approach. Statistics of the putative contaminant sequences are presented in Additional file 3: Supplementary Table 23. Genes were predicted in the putative contaminant sequences using PROKKA [76]

(v1.13.3; --metagenome) and annotated with protein domains identified using *pfam\_scan.pl* (v1.6; Pfam database release 31) at  $E$  value  $< 0.001$  following earlier studies [15, 47, 77].

#### Identification and removal of organelle sequences

The coding sequences from the plastid genome of *Cladocopium* sp. C3 (formerly *Symbiodinium* subtype C3) were used to identify putative plastid sequences from the assembly [78]. A scaffold was considered to be putatively of plastid origin if it shared significant sequence similarity (BLASTN) to one of the above sequences, covering  $> 75\%$  the sequence length at  $E \leq 10^{-10}$ .

The complete CDS of *cox1*, *cox3*, and *cob* from *Breviolum minutum* (LC002801.1 and LC002802.1) were retrieved (because no complete sequences yet exist for *Polarella glacialis*) and used to identify putative mitochondrial scaffolds (see Additional file 1: Supplementary Note, and Additional file 3: Supplementary Table 24). A scaffold was considered putative mitochondrial if it shared significant similarity (BLASTN, max\_target\_seqs 10,000) to one of the above sequences, covering  $> 75\%$  of the sequence length at  $E \leq 10^{-10}$ . Statistics of the putative mitochondrial and plastidic sequences are presented in Additional file 3: Supplementary Table 23.

#### Customised gene prediction workflow tailored for dinoflagellate genomes

To predict protein-coding genes, an ab initio gene prediction approach adapted from Liu et al. [12] was applied to the genomes of *P. glacialis*; this approach, also reported in Chen et al. [39], is available at [https://github.com/TimothyStephens/Dinoflagellate\\_Annotation\\_Workflow](https://github.com/TimothyStephens/Dinoflagellate_Annotation_Workflow). For each genome assembly, a de novo repeat library was first derived using RepeatModeler v1.0.11 (<http://www.repeatmasker.org/RepeatModeler/>). All repeats (including known repeats in RepeatMasker database release 20170127) were masked using RepeatMasker v4.0.7 (<http://www.repeatmasker.org/>).

We used transcriptome data generated in this study to guide gene prediction of assembled genomes. For RNA-Seq data, we assembled the reads using Trinity [79] independently in 'de novo' mode (v2.6.6) and 'genome-guided' mode (v2.8.4); the assembled transcriptomes are very similar between the two isolates (Additional file 3: Supplementary Table 25), and almost all RNA-Seq reads mapped onto the corresponding genome assemblies (Additional file 3: Supplementary Table 21). The combined Trinity assemblies were trimmed using SeqClean (<https://sourceforge.net/projects/seqclean/>). The RNA-Seq and polished PacBio IsoSeq transcripts were combined into gene assemblies using PASA v2.3.3 [38] that was customised (available at <https://github.com/chancx/dinoflag-alt-splice>) to recognise an additional donor

splice site (GA). TransDecoder v5.2.0 [38] was used to predict open reading frames on the PASA assembled transcripts. Complete proteins (CDS with both start and stop codons) predicted by TransDecoder that had valid genome coordinates and more than one exon were retained for further analysis.

These proteins were searched (BLASTP,  $E \leq 10^{-20}$ ) against a customised protein database that consists of RefSeq proteins release 88 and other predicted Symbiodiniaceae and *Polarella* proteins (see Additional file 3: Supplementary Table 26). Only nearly full-length proteins were included in the subsequent analysis; we defined nearly full-length proteins as sequences with a BLAST hit that covered  $> 80\%$  of both the query and subject sequences.

The nearly full-length gene models were checked for TEs using HHblits v2.0.16 [80] (-p 80 -e 1E-5 -E 1E-5) searching against the JAMg transposon database (<https://sourceforge.net/projects/jamg/files/databases/>), as well as with Transposon-PSI (<http://transposonpsi.sourceforge.net/>). Gene models containing TEs were removed from the gene set, and redundancy reduction was conducted using CD-HIT v4.6.8 [81] (ID = 75%; -c 0.75 -n 5). The remaining gene models were processed using the Prepare\_golden\_genes\_for\_predictors.pl (<http://jamg.sourceforge.net/>) script from the JAMg pipeline (altered to recognise GA donor splice sites). This script produces a set of 'golden genes', which were used as a training set for the gene prediction tools AUGUSTUS v3.3.1 [82] and SNAP version 2006-07-28 [83]. We used a customised code of AUGUSTUS (available at <https://github.com/chancx/dinoflag-alt-splice>), so it recognises GA donor splice sites, and trained it to predict both coding sequences and untranslated regions; SNAP was trained for both GT and GC donor splice sites. Soft-masked genomes were passed to GeneMark-ES [84] for training and gene prediction.

UniProt-SwissProt (retrieved 27/06/2018) proteins and other predicted Symbiodiniaceae and *Polarella* proteins (see Additional file 3: Supplementary Table 26) were combined to produce a set of gene models using MAKER v2.31.8 (altered to recognise GA donor splice sites) [85] in protein2genome mode; the custom repeat library was used by RepeatMasker as part of MAKER prediction. Two sets of predicted protein-coding genes, one derived using the RNA-Seq data and one using the IsoSeq data, were constructed using PASA (--ALT\_SPLICE -N 2) and TransDecoder (ORF prediction guided by Pfam database release 31). Gene models constructed using the IsoSeq data were assumed to be full-length, and an extra step was taken to correct predicted proteins produced by TransDecoder that were five-prime partial. If a protein had an in-frame start codon within either the first 30 positions or the first 30% of the



sequence, that position was then considered as the start of that sequence. Sequences not satisfying these criteria were left unchanged. A primary set of predicted genes was produced using EvidenceModeler v1.1.1 [86], which had been altered to recognise GA donor splice sites. This tool combined the gene models from PASA RNA-Seq, PASA IsoSeq (with corrected start positions where applicable), AUGUSTUS, MAKER protein2genome, and GeneMark-ES to a single set of evidence-based predictions. EvidenceModeler was allowed to predict genes within introns of other genes if the intron was >10,000 bp (--search\_long\_introns 10000).

Unlike Liu et al. [12], we did not incorporate gene predictions from the SNAP program into the EvidenceModeler stage of the prediction workflow. This was done because SNAP produced an excessive number of overlapping genes that were encoded on opposite strands. As genes encoded in this manner were not found to be supported in the transcriptome, we decided to exclude the results of this program from our predictions. We did not provide the location of putative repetitive elements to EvidenceModeler either, as multi-copy genes are often classified as repeats by RepeatModeler and would have been excluded from our final gene set. The weightings used for integration of gene models with EvidenceModeler were PASA IsoSeq (with corrected start sites) 15, PASA RNA-Seq 10, Maker protein2genome 4, AUGUSTUS 1, and GeneMark-ES 1. EvidenceModeler gene models were considered high-confidence if they had been constructed using evidence either from PASA inputs or from  $\geq 2$  other prediction methods.

The transcriptome support shown in Additional file 3: Supplementary Table 12 was calculated for each *P. glacialis* isolate by searching the high-confidence EvidenceModeler genes against a database of all RNA-Seq and IsoSeq transcripts (from the same isolate) using BLASTN. Genes were considered to have transcriptome support if they had a hit with >90% identity that covered >50% of the gene.

In addition, rRNA sequences were predicted using RNAmmer v1.2 (-S euk) [87], and tRNA sequences were predicted using tRNAscan-SE v2.0.5 (-H -y -detail) [45]. High-confidence tRNA predictions were obtained using the EukHighConfidenceFilter (-r) script that is distributed as part of the tRNAscan package.

#### Functional annotation of predicted genes

Protein domains were searched using pfam\_scan.pl (v1.6; Pfam database release 31) at  $E$  value <0.001 following earlier studies [15, 47, 77]. Where required, proteins were queried using BLASTP against SwissProt and TrEMBL databases (UniProt release 2018\_02) independently. Only the hits from the top 20 target sequences from each search were retained if  $E \leq 10^{-5}$ . Gene

Ontology (GO; <http://geneontology.org/>) terms were assigned using the UniProt-GOA mapping (release 2019\_05\_07) database and the best UniProt hit with associated GO terms for each sequence.

Pfam domains in *P. glacialis* was assessed for enrichment against a background set using Fisher's exact test, with correction for multiple testing using the Benjamini and Hochberg method [88]; a  $p$  value  $\leq 0.05$  is considered significant. GO enrichment was conducted using the topGO R (v2.34.0) [89] package, applying Fisher's exact test with the 'elimination' methods to correct for the hierarchical structure of GO terms. The background used consisted of the available Symbiodiniaceae genomes (*Symbiodinium microadriaticum* [13], *Breviolum minutum* [14], *Cladocopium goreauii* [12], *Fugacium kawagutii* [12], *Symbiodinium tridacnidorum* [15], and *Cladocopium* sp. C92 [15]) with the revised gene predictions from Chen et al. [39].

#### Analysis of completeness of assembled genomes and predicted proteins

Completeness of the predicted genes in *P. glacialis* was assessed using BUSCO v3.1.0 (--mode proteins) [90] with the alveolate\_stramenophiles\_ensembl, Eukaryota\_odb9, and protists\_ensembl datasets (retrieved 22 September 2017); BLASTP searches ( $E \leq 10^{-5}$ ) using the same three BUSCO datasets; and BLASTP searches ( $E \leq 10^{-5}$ ) using the protein orthologs from the Core Eukaryotic Genes dataset [26] (see Additional file 3: Supplementary Table 5).

Completeness of the assembled genomes of *P. glacialis* was assessed using BUSCO v3.1.0 (--mode proteins) [90] and TBLASTN searches ( $E \leq 10^{-5}$ ) using the same three BUSCO datasets and TBLASTN searches ( $E \leq 10^{-5}$ ) using the protein orthologs from the Core Eukaryotic Genes dataset [26] (see Additional file 3: Supplementary Table 5). The modified version of Augustus used for the gene prediction was used for the BUSCO analysis as well.

#### Identification of *P. glacialis* sequences in the TARA database

The Ocean Microbial Reference Gene Catalogue was retrieved from [ftp://ftp.sra.ebi.ac.uk/vol1/ERA412/ERA412970/tab/OM-RGC\\_seq\\_release.tsv.gz](ftp://ftp.sra.ebi.ac.uk/vol1/ERA412/ERA412970/tab/OM-RGC_seq_release.tsv.gz). Genes classified as being from 'Dinophyceae' or that were from the kingdom 'undef' were extracted and searched against the genome of both *P. glacialis* isolates using BLASTN (at default parameters). Genes (i.e. the query) were retained if they had a hit in the genome sequences, in which the aligned region covered >75% of the query length at >95% identity. The retained genes were then searched against the non-redundant (nr) nucleotide database at

NCBI for further verification of their origins (20 May 2019). No *P. glacialis* sequences were identified this way.

#### Comparison of predicted proteins and genome sequence similarity between *P. glacialis* isolates

Comparison between the protein sequences of CCMP1383 and CCMP2088 was conducted using BLASTP ( $E \leq 10^{-5}$ ; Fig. 3a). For each isolate, protein sequences that do not share similarity to those of the counterpart isolate were identified. For these proteins, the corresponding coding gene sequences were searched (BLASTN) against the transcripts of the counterpart isolate; we consider a shared sequence similarity of >90% identity covering >50% of the query as significant. Tandem repeated genes were identified with MScanX [91] (intra-species; -b 1) using hits from BLASTP ( $E \leq 10^{-10}$ ) with query or subject coverage >50%.

Sequence similarity between the genomes of the *P. glacialis* isolates was assessed using non-repeat regions of the genome. Repeat features predicted using RepeatModeler and RepeatMasker were excluded from the analysis; regions between repeats that were  $\leq 10$  bp of each other were also removed. From the remaining non-repetitive regions, only those  $\geq 100$  bp and with  $\leq 10$  ambiguous ('N') bases were used as query in a BLASTN (-dust no,  $E \leq 10^{-10}$ ) search against the genome of the other isolate. The top hit of each sequence was retained for further analysis.

#### Analysis of tandemly repeated gene blocks encoding PCP, bacteriorhodopsin, and ice-binding domain

For each tandemly repeated block encoding the same gene function, we assessed the sequence similarity among the coded protein sequences, and at the DNA level, the coding sequence regions, and the intergenic regions. For each block, alignments of coded proteins were identified using BLASTP ( $E \leq 10^{-5}$ ) searches, and for the coding regions and intergenic regions, sequence alignments were identified using BLASTN ( $E \leq 10^{-5}$ ) searches; self-matches were ignored. In each case (of proteins, coding regions, and intergenic regions), the mean percent identity ( $x$ ) of all alignments within a block was computed. Over all blocks that encode the same gene function, the mean and standard deviation, and the minimum and maximum values of  $x$  were computed.

#### Inference of homologous protein sets among *Suessiales*

Putatively homologous protein sets were constructed using OrthoFinder v2.3.3 (inflation 1.5) [92] with sequence similarity computed with DIAMOND v0.9.24 [93]. We defined dark homologous protein sets using the same criteria as Stephens et al. [47] but excluding hits from any sequences with functions described as 'uncharacterized'.

#### Functional classification of rhodopsin

Predicted proteins of *P. glacialis* with top hits described as 'rhodopsin' in UniProt were retrieved. The specific type for each identified *P. glacialis* rhodopsin was identified using a BLASTP ( $E \leq 10^{-5}$ ) search against the known proton-pump (ABV22426, ADY17811) and sensory type (ADY17810, KF651052, KF651053, KF651054, KF651055) sequences from *Oxyrrhis marina*. The top hit for each query sequence was used to assign type.

#### Phylogenetic inference of DUF3494 domains

A comprehensive set of DUF3494 domain-encoding proteins was collected from the transcriptomes of *Heterocapsa arctica* CCMP445, *Peridinium aciculiferum* PAER\_2, *Scrippsiella hangoei* like-SHHI\_4, and *Scrippsiella hangoei* SHTV5 (retrieved from Microbial Eukaryote Transcriptome Sequencing Project (MMETSP) [94]) for comparison against those predicted in both *P. glacialis* isolates. Predicted DUF3494-encoding proteins from the bacteria associated with *P. glacialis* were found with pfam\_scan.pl (see above). DUF3494 domain regions were extracted from the proteins if they covered >50% the length of the Pfam DUF3494 domain HMM. DUF3494 domains from the Pfam\_Full dataset (retrieved 14 April 2019) were retrieved. Identical sequences within each dataset were removed using cd-hit (-c 1.00 -n 5) [81]. All DUF3494 domains and domain regions were aligned using MAFFT v7.407 (--localpair --maxiterate 1000) [95], from which a maximum likelihood tree was constructed using IQ-TREE v1.6.10 (-m MFP -msub nuclear -bb 2000 -nm 2000) [96, 97]. Support of nodes in the inferred tree was determined using 2000 ultrafast bootstraps [60].

#### Analysis of simple repeats and multi-copy genes

The de novo repeat families identified by RepeatModeler during gene prediction were scrutinised for the presence of multi-copy genes. Unclassified repeat families (type unknown) were compared using BLASTN ( $E \leq 10^{-5}$ ) against the final gene models. Queries (repeat families) with >80% of their sequence, or the sequence of the subject (predicted genes), being covered in the BLAST hit were retained. This strategy (considering cover of both query and subject) is designed to capture cases where either the whole repeat is contained within a gene (repetitive exon) or a whole gene is contained within a larger repeat.

To specifically assess the presence of simple repeats in the assembled genomes, RepeatMasker was re-run on each genome using the default library (RepeatMasker database release 20170127) searching for just simple repeats (-noint). Repeats of type (TTG) $n$ , (TGT) $n$ , (GTT) $n$ , (AAC) $n$ , (ACA) $n$ , and (CAA) $n$  are all derived from the same pattern and thus are considered interchangeable for the purposes of this study. Overlapping



repeats of these types were merged, and their total length was reported as the coverage of the TTG repeat. 3-mers were extracted from the cleaned genome assembly using `kmercountexact.sh` from the `bbmaps` tool suite (see Additional file 3: Supplementary Table 6). The quality trimmed and merged genome reads were sampled at 5% before 3-mers were extracted (`reformat.sh` `sample-rate=0.05`, 3-mers extracted using `kmercountexact.sh`). This was done to prevent 3-mer counts from exceeding the maximum value a 32-bit integer can store.

### Analysis of spliced leader sequences

Polished PacBio IsoSeq sequences that contained the dinoflagellate spliced leader sequence (CCGTAGCCATTTGGCTCAAG) were identified using BLASTN (`-max_target_seqs 1000000 -task blastn-short -evalue 1000`). Only sequences with hits that start  $\leq 5$  bp from their 5'-end, ended  $\geq 20$  bp along the DinoSL sequence, and had zero gap openings and a maximum of one mismatch were considered to contain the spliced leader sequence. Relic DinoSL sequences were identified by BLASTN (`-max_target_seqs 1000000 -task blastn-short -evalue 1000`), using the full DinoSL and a relic sequence joined together as the query [32]. Multiple relic DinoSL were identified using the full DinoSL and multiple relic DinoSL sequences joined together. Sequences were considered to contain a relic DinoSL if they had a hit that started within the first 11 bases of the query sequence (allows for truncation of the transcript), within the first 5 bases of the transcript, and finished within 5 bases of the end of the query sequence.

### Supplementary information

Supplementary information accompanies this paper at <https://doi.org/10.1186/s12915-020-00782-8>.

**Additional file 1:** Supplementary Note.

**Additional file 2:** Supplementary Figures 1 through 5.

**Additional file 3:** Supplementary Tables 1 through 26.

**Additional file 4:** Supplementary Data. The complete phylogenetic tree of ice-binding domains in NEWICK format.

### Acknowledgements

This project was supported by the computational resources of the National Computational Infrastructure (NCI) National Facility systems through the NCI Merit Allocation Scheme (Project d85) awarded to CXC and MAR. We thank Professor Ben Hankamer and Dr Melanie Oey for providing and facilitating our access to the algal culturing lab and facility at the University of Queensland's Institute for Molecular Bioscience.

### Authors' contributions

TGS, MAR, and CXC conceived the study. TGS, RAGP, CXC, MAR, DB, and DWB designed the analyses and interpreted the results. CXC maintained the dinoflagellate cultures. CXC and ARM extracted the biological materials for sequencing. YC generated the long-read libraries for genome and full-length transcriptome sequencing. TGS conducted all the computational analyses, prepared all the figures and tables, and prepared the first draft of the

manuscript. All authors prepared, wrote, reviewed, commented on, and approved the final manuscript.

### Funding

TGS was supported by an Australian Government Research Training Program (RTP) Scholarship. DWB and YC are supported by a Human Frontier Science Program grant (RGP0030). This project was supported by two Australian Research Council grants (DP150101875 awarded to MAR, CXC, and DB, and DP190102474 awarded to CXC and DB). DB was supported by a NIFA-USDA Hatch grant (NJ01170). All funding bodies have no roles in the design of the study; collection, analysis, and interpretation of the data; and writing of the manuscript.

### Availability of data and materials

All data generated or analysed during this study are included in this published article and its supplementary information files. All sequence data generated from this study are available at the NCBI Short Read Archive (SRA) BioProject accession PRJEB33539, with SRA accessions ERS3790104 and ERS3790106 for CCMP1383, and ERS3790105 and ERS3790107 for CCMP2088. The assembled genomes, predicted gene models and proteins from both *P. glacialis* isolates are available at <https://doi.org/10.14264/uq.2020.222>.

### Ethics approval and consent to participate

Not applicable.

### Consent for publication

Not applicable.

### Competing interests

The authors declare that they have no competing interests.

### Author details

<sup>1</sup>Institute for Molecular Bioscience, The University of Queensland, Brisbane, QLD 4072, Australia. <sup>2</sup>Present Address: Department of Biochemistry and Microbiology, Rutgers University, New Brunswick, NJ 08901, USA. <sup>3</sup>Present address: Department of Integrative Biology, University of South Florida, Tampa, FL 33620, USA. <sup>4</sup>UQ Genomics Initiative, The University of Queensland, Brisbane, QLD 4072, Australia. <sup>5</sup>Present Address: Faculty of Science, School of Life and Environmental Sciences, The University of Sydney, Camperdown, NSW 2006, Australia. <sup>6</sup>Commonwealth Scientific and Industrial Research Organisation (CSIRO) Agriculture and Food, Queensland Bioscience Precinct, Brisbane, QLD 4067, Australia. <sup>7</sup>UQ Genomics, The University of Queensland, Brisbane, QLD 4072, Australia. <sup>8</sup>Department of Biochemistry and Microbiology, Rutgers University, New Brunswick, NJ 08901, USA. <sup>9</sup>School of Chemistry and Molecular Biosciences, The University of Queensland, Brisbane, QLD 4072, Australia. <sup>10</sup>Australian Centre for Ecogenomics, The University of Queensland, Brisbane, QLD 4072, Australia.

Received: 3 November 2019 Accepted: 20 April 2020

Published online: 24 May 2020

### References

1. Guiry MD. How many species of algae are there? *J Phycol.* 2012;48(5):1057–63.
2. Fensome RA, MacRae RA, Moldovan JM, Taylor FJR, Williams GL. The early Mesozoic radiation of dinoflagellates. *Paleobiology.* 2016;22(3):329–38.
3. Baker AC. Flexibility and specificity in coral-algal symbiosis: diversity, ecology, and biogeography of *Symbiodinium*. *Annu Rev Ecol Syst.* 2003;34(1):661–89.
4. LaJeunesse TC, Parkinson JE, Gabrielson PW, Jeong HJ, Reimer JD, Voolstra CR, Santos SR. Systematic revision of Symbiodiniaceae highlights the antiquity and diversity of coral endosymbionts. *Curr Biol.* 2018;28(16):2570–80.
5. Stentiford GD, Shields JD. A review of the parasitic dinoflagellates *Hematodinium* species and *Hematodinium*-like infections in marine crustaceans. *Dis Aquat Org.* 2005;66(1):47–70.
6. Grattan LM, Holobaugh S, Morris JG Jr. Harmful algal blooms and public health. *Harmful Algae.* 2016;57(Pt B):2–8.
7. Taylor FJR, Hoppenrath M, Saldarriaga JF. Dinoflagellate diversity and distribution. *Biodivers Conserv.* 2008;17(2):407–18.
8. Gómez F. A quantitative review of the lifestyle, habitat and trophic diversity of dinoflagellates (Dinoflagellata, Alveolata). *Syst Biodivers.* 2012;10(3):267–75.

9. Le Bescot N, Mahé F, Audic S, Dimier C, Garet MJ, Poulain J, Wincker P, de Vargas C, Siano R. Global patterns of pelagic dinoflagellate diversity across protist size classes unveiled by metabarcoding. *Environ Microbiol.* 2016; 18(2):609–26.
10. Montresor M, Proccaccini G, Stoecker DK. *Polarella glacialis*, gen. nov., sp. nov. (Dinophyceae): Suessiaceae are still alive! *J Phycol.* 1999;35(1):186–97.
11. Lin S, Cheng S, Song B, Zhong X, Lin X, Li W, Li L, Zhang Y, Zhang H, Ji Z, et al. The *Symbiodinium kawagutii* genome illuminates dinoflagellate gene expression and coral symbiosis. *Science.* 2015;350(6261):691–4.
12. Liu H, Stephens TG, González-Pech RA, Beltran VH, Lapeyre B, Bongaerts P, Cooke I, Aranda M, Bourne DG, Forêt S, et al. *Symbiodinium* genomes reveal adaptive evolution of functions related to coral-dinoflagellate symbiosis. *Commun Biol.* 2018;1:95.
13. Aranda M, Li Y, Liew YJ, Baumgarten S, Simakov O, Wilson MC, Piel J, Ashoor H, Bougouffa S, Bajic VB, et al. Genomes of coral dinoflagellate symbionts highlight evolutionary adaptations conducive to a symbiotic lifestyle. *Sci Rep.* 2016;6:39734.
14. Shoguchi E, Shinzato C, Kawashima T, Gyoja F, Mungpakdee S, Koyanagi R, Takeuchi T, Hisata K, Tanaka M, Fujiwara M, et al. Draft assembly of the *Symbiodinium minutum* nuclear genome reveals dinoflagellate gene structure. *Curr Biol.* 2013;23(15):1399–408.
15. Shoguchi E, Beedesse G, Tada I, Hisata K, Kawashima T, Takeuchi T, Arakaki N, Fujie M, Koyanagi R, Roy MC, et al. Two divergent *Symbiodinium* genomes reveal conservation of a gene cluster for sunscreen biosynthesis and recently lost genes. *BMC Genomics.* 2018;19(1):458.
16. John U, Lu Y, Wohlrab S, Groth M, Janouškovec J, Kohli GS, Mark FC, Bickmeyer U, Farhat S, Felder M, et al. An aerobic eukaryotic parasite with functional mitochondria that likely lacks a mitochondrial genome. *Sci Adv.* 2019;5(4):eaav1110.
17. Gornik SG, Febrimarsa, Cassin AM, MacRae JJ, Ramaprasad A, Rchiad Z, McConville MJ, Bacic A, McFadden GI, Pain A, et al. Endosymbiosis undone by stepwise elimination of the plastid in a parasitic dinoflagellate. *Proc Natl Acad Sci U S A.* 2015;112(18):5767–72.
18. Lajeunesse TC, Lambert G, Andersen RA, Coffroth MA, Galbraith DW. *Symbiodinium* (Pyrrhophyta) genome sizes (DNA content) are smallest among dinoflagellates. *J Phycol.* 2005;41(4):880–6.
19. Allen JR, Roberts M, Loeblich AR III, Klotz LC. Characterization of the DNA from the dinoflagellate *Cryptothecodinium cohnii* and implications for nuclear organization. *Cell.* 1975;6(2):161–9.
20. Jaekisch N, Yang J, Wohlrab S, Glöckner G, Kroymann J, Vogel H, Cembella A, John U. Comparative genomic and transcriptomic characterization of the toxigenic marine dinoflagellate *Alexandrium ostenfeldii*. *PLoS One.* 2011; 6(12):e28012.
21. Le QH, Markovic P, Hastings JW, Jovine RV, Morse D. Structure and organization of the peridinin-chlorophyll *a*-binding protein gene in *Gonyaulax polyedra*. *Mol Gen Genomics.* 1997;255(6):595–604.
22. Montresor M, Lovejoy C, Orsini L, Proccaccini G, Roy S. Bipolar distribution of the cyst-forming dinoflagellate *Polarella glacialis*. *Polar Biol.* 2003;26(3):186–94.
23. Cuadrado A, De Bustos A, Figueroa RI. Chromosomal markers in the genus *Karenia*: towards an understanding of the evolution of the chromosomes, life cycle patterns and phylogenetic relationships in dinoflagellates. *Sci Rep.* 2019;9(1):3072.
24. Bouligand Y, Norris V. Chromosome separation and segregation in dinoflagellates and bacteria may depend on liquid crystalline states. *Biochimie.* 2001;83(2):187–92.
25. Lin S. Genomic understanding of dinoflagellates. *Res Microbiol.* 2011;162(6): 551–69.
26. Parra G, Bradnam K, Ning Z, Keane T, Korf I. Assessing the gene space in draft genomes. *Nucleic Acids Res.* 2009;37(1):289–97.
27. McEwan M, Humayun R, Slamovits CH, Keeling PJ. Nuclear genome sequence survey of the dinoflagellate *Heterocapsa triquetra*. *J Eukaryot Microbiol.* 2008;55(6):530–5.
28. Ponmani T, Guo R, Ki JS. Analysis of the genomic DNA of the harmful dinoflagellate *Prorocentrum minimum*: a brief survey focused on the noncoding RNA gene sequences. *J Appl Phycol.* 2016;28(1):335–44.
29. Kimura M. A simple method for estimating evolutionary rates of base substitutions through comparative studies of nucleotide sequences. *J Mol Evol.* 1980;16(2):111–20.
30. Galindo-González L, Mhiri C, Deyholos MK, Grandbastien MA. LTR-retrotransposons in plants: engines of evolution. *Gene.* 2017;626:14–25.
31. Zhang H, Hou Y, Miranda L, Campbell DA, Sturm NR, Gaasterland T, Lin S. Spliced leader RNA trans-splicing in dinoflagellates. *Proc Natl Acad Sci U S A.* 2007;104(11):4618–23.
32. Slamovits CH, Keeling PJ. Widespread recycling of processed cDNAs in dinoflagellates. *Curr Biol.* 2008;18(13):R550–2.
33. Zhang H, Campbell DA, Sturm NR, Lin S. Dinoflagellate spliced leader RNA genes display a variety of sequences and genomic arrangements. *Mol Biol Evol.* 2009;26(8):1757–71.
34. Zemach A, Zilberman D. Evolution of eukaryotic DNA methylation and the pursuit of safer sex. *Curr Biol.* 2010;20(17):R780–5.
35. Lohuis MR, Miller DJ. Hypermethylation at CpG-motifs in the dinoflagellates *Amphidinium carterae* (Dinophyceae) and *Symbiodinium microadriaticum* (Dinophyceae): evidence from restriction analyses, 5-azacytidine and ethionine treatment. *J Phycol.* 1998;34(1):152–9.
36. Law JA, Jacobsen SE. Establishing, maintaining and modifying DNA methylation patterns in plants and animals. *Nat Rev Genet.* 2010;11(3):204–20.
37. de Mendoza A, Bonnet A, Vargas-Landini DB, Ji N, Li H, Yang F, Li L, Hori K, Pflueger J, Buckberry S, et al. Recurrent acquisition of cytosine methyltransferases into eukaryotic retrotransposons. *Nat Commun.* 2018; 9(1):1341.
38. Haas BJ, Delcher AL, Mount SM, Wortman JR, Smith RK, Hannick LI, Maiti R, Ronning CM, Rusch DB, Town CD, et al. Improving the *Arabidopsis* genome annotation using maximal transcript alignment assemblies. *Nucleic Acids Res.* 2003;31(19):5654–66.
39. Chen Y, González-Pech RA, Stephens TG, Bhattacharya D, Chan CX. Evidence that inconsistent gene prediction can mislead analysis of dinoflagellate genomes. *J Phycol.* 2020;56(1):6–10.
40. Liew YJ, Li Y, Baumgarten S, Voolstra CR, Aranda M. Condition-specific RNA editing in the coral symbiont *Symbiodinium microadriaticum*. *PLoS Genet.* 2017;13(2):e1006619.
41. Klinger CM, Paoli L, Newby RJ, Wang MY-W, Carroll HD, Leblond JD, Howe CJ, Dacks JB, Bowler C, Cahoon AB, et al. Plastid transcript editing across dinoflagellate lineages shows lineage-specific application but conserved trends. *Genome Biol Evol.* 2018;10(4):1019–38.
42. Lin S, Zhang H, Spencer DF, Norman JE, Gray MW. Widespread and extensive editing of mitochondrial mRNAs in dinoflagellates. *J Mol Biol.* 2002;320(4):727–39.
43. Mungpakdee S, Shinzato C, Takeuchi T, Kawashima T, Koyanagi R, Hisata K, Tanaka M, Goto H, Fujie M, Lin S, et al. Massive gene transfer and extensive RNA editing of a symbiotic dinoflagellate plastid genome. *Genome Biol Evol.* 2014;6(6):1408–22.
44. Michaud M, Cognat V, Duchêne AM, Maréchal-Drouard L. A global picture of tRNA genes in plant genomes. *Plant J.* 2011;66(1):80–93.
45. Chan PP, Lowe TM. tRNAscan-SE: searching for tRNA genes in genomic sequences. *Methods Mol Biol.* 1962;2019:1–14.
46. Srivastava AK, Schlessinger D. Structure and organization of ribosomal DNA. *Biochimie.* 1991;73(6):631–8.
47. Stephens TG, Ragan MA, Bhattacharya D, Chan CX. Core genes in diverse dinoflagellate lineages include a wealth of conserved dark genes with unknown functions. *Sci Rep.* 2018;8(1):17175.
48. Beauchemin M, Roy S, Daoust P, Dagenais-Bellefeuille S, Bertomeu T, Letourneau L, Lang BF, Morse D. Dinoflagellate tandem array gene transcripts are highly conserved and not polycistronic. *Proc Natl Acad Sci U S A.* 2012;109(39):15793–8.
49. Reichman JR, Wilcox TP, Vize PD. PCP gene family in *Symbiodinium* from *Hippopus hippopus*: low levels of concerted evolution, isoform diversity, and spectral tuning of chromophores. *Mol Biol Evol.* 2003;20(12):2143–54.
50. Bachvaroff TR, Place AR. From stop to start: tandem gene arrangement, copy number and trans-splicing sites in the dinoflagellate *Amphidinium carterae*. *PLoS One.* 2008;3(8):e2929.
51. Lin S, Zhang H, Zhuang Y, Tran B, Gill J. Spliced leader-based metatranscriptomic analyses lead to recognition of hidden genomic features in dinoflagellates. *Proc Natl Acad Sci U S A.* 2010;107(46):20033–8.
52. Slamovits CH, Okamoto N, Burri L, James ER, Keeling PJ. A bacterial proteorhodopsin proton pump in marine eukaryotes. *Nat Commun.* 2011;2: 183.
53. Béjà O, Spudich EN, Spudich JL, Leclerc M, DeLong EF. Proteorhodopsin phototrophy in the ocean. *Nature.* 2001;411(6839):786–9.
54. Fuhrman JA, Schwalbach MS, Stingl U. Proteorhodopsins: an array of physiological roles? *Nat Rev Microbiol.* 2008;6(6):488–94.

55. Shi X, Li L, Guo C, Lin X, Li M, Lin S. Rhodopsin gene expression regulated by the light dark cycle, light spectrum and light intensity in the dinoflagellate *Prorocentrum*. *Front Microbiol.* 2015;6:555.
56. Marchetti A, Schrueth DM, Durkin CA, Parker MS, Kodner RB, Berthiaume CT, Morales R, Allen AE, Armbrust EV. Comparative metatranscriptomics identifies molecular bases for the physiological responses of phytoplankton to varying iron availability. *Proc Natl Acad Sci U S A.* 2012;109(6):E317–25.
57. Guo Z, Zhang H, Lin S. Light-promoted rhodopsin expression and starvation survival in the marine dinoflagellate *Oxryrhis marina*. *PLoS One.* 2014;9(12):e114941.
58. Jiang J, Zhang H, Kang Y, Bina D, Lo CS, Blankenship RE. Characterization of the peridinin-chlorophyll *a*-protein complex in the dinoflagellate *Symbiodinium*. *Biochim Biophys Acta.* 2012;1817(7):983–9.
59. Vance TDR, Bayer-Giraldi M, Davies PL, Mangiagalli M. Ice-binding proteins and the 'domain of unknown function' 3494 family. *FEBS J.* 2019;286(5):855–73.
60. Hoang DT, Chernomor O, von Haeseler A, Minh BQ, Vinh LS. UFBoot2: improving the ultrafast bootstrap approximation. *Mol Biol Evol.* 2018;35(2):518–22.
61. Arai T, Fukami D, Hoshino T, Kondo H, Tsuda S. Ice-binding proteins from the fungus *Antarctomyces psychrotrophicus* possibly originate from two different bacteria through horizontal gene transfer. *FEBS J.* 2019;286(5):946–62.
62. Sorhannus U. Evolution of antifreeze protein genes in the diatom genus *Fragilariopsis*: evidence for horizontal gene transfer, gene duplication and episodic diversifying selection. *Evol Bioinformatics Online.* 2011;7:279–89.
63. Nash EA, Barbrook AC, Edwards-Stuart RK, Bernhardt K, Howe CJ, Nisbet RE. Organization of the mitochondrial genome in the dinoflagellate *Amphidinium carterae*. *Mol Biol Evol.* 2007;24(7):1528–36.
64. Yin J, Chen J, Liu G, Yu Y, Song L, Wang X, Qu X. Complete genome sequence of *Glacielcola psychrophila* strain 170T. *Genome Announc.* 2013;1(3):e00199–13.
65. Shinzato C, Hisata K, Satoh N, Mungpakdee S, Shoguchi E. The large mitochondrial genome of *Symbiodinium minutum* reveals conserved noncoding sequences between dinoflagellates and apicomplexans. *Genome Biol Evol.* 2015;7(8):2237–44.
66. Guillard RRL, Ryther JH. Studies of marine planktonic diatoms: I. *Cyclotella nana* Hustedt, and *Detonula confervacea* (Cleve) Gran. *Can J Microbiol.* 1962;8(2):229–39.
67. Bolger AM, Lohse M, Usadel B. Trimmomatic: a flexible trimmer for Illumina sequence data. *Bioinformatics.* 2014;30(15):2114–20.
68. Magoc T, Salzberg SL. FLASH: fast length adjustment of short reads to improve genome assemblies. *Bioinformatics.* 2011;27(21):2957–63.
69. Leggett RM, Clavijo BJ, Clissold L, Clark MD, Caccamo M. NextClip: an analysis and read preparation tool for Nextera Long Mate Pair libraries. *Bioinformatics.* 2014;30(4):566–8.
70. Langmead B, Salzberg SL. Fast gapped-read alignment with Bowtie 2. *Nat Methods.* 2012;9(4):357–9.
71. Marçais G, Kingsford C. A fast, lock-free approach for efficient parallel counting of occurrences of *k*-mers. *Bioinformatics.* 2011;27(6):764–70.
72. Vurture GW, Sedlazeck FJ, Nattestad M, Underwood CJ, Fang H, Gurtowski J, Schatz MC. GenomeScope: fast reference-free genome profiling from short reads. *Bioinformatics.* 2017;33(14):2202–4.
73. Pryszcz LP, Gabaldón T. Redundans: an assembly pipeline for highly heterozygous genomes. *Nucleic Acids Res.* 2016;44(12):e113.
74. Zimin AV, Puiu D, Luo MC, Zhu T, Koren S, Marçais G, Yorke JA, Dvořák J, Salzberg SL. Hybrid assembly of the large and highly repetitive genome of *Aegilops tauschii*, a progenitor of bread wheat, with the MaSuRCA mega-reads algorithm. *Genome Res.* 2017;27(5):787–92.
75. Roach MJ, Schmidt SA, Borneman AR. Purge Haplotigs: allelic contig reassignment for third-gen diploid genome assemblies. *BMC Bioinformatics.* 2018;19(1):460.
76. Seemann T. Prokka: rapid prokaryotic genome annotation. *Bioinformatics.* 2014;30(14):2068–9.
77. González-Pech RA, Ragan MA, Chan CX. Signatures of adaptation and symbiosis in genomes and transcriptomes of *Symbiodinium*. *Sci Rep.* 2017;7(1):15021.
78. Barbrook AC, Voolstra CR, Howe CJ. The chloroplast genome of a *Symbiodinium* sp. clade C3 isolate. *Protist.* 2014;165(1):1–13.
79. Grabherr MG, Haas BJ, Yassour M, Levin JZ, Thompson DA, Amit I, Adiconis X, Fan L, Raychowdhury R, Zeng Q, et al. Full-length transcriptome assembly from RNA-Seq data without a reference genome. *Nat Biotechnol.* 2011;29(7):644–52.
80. Remmert M, Biegert A, Hauser A, Söding J. HHblits: lightning-fast iterative protein sequence searching by HMM-HMM alignment. *Nat Methods.* 2011;9(2):173–5.
81. Li W, Godzik A. Cd-hit: a fast program for clustering and comparing large sets of protein or nucleotide sequences. *Bioinformatics.* 2006;22(13):1658–9.
82. Stanke M, Keller O, Gunduz I, Hayes A, Waack S, Morgenstern B. AUGUSTUS: ab initio prediction of alternative transcripts. *Nucleic Acids Res.* 2006;34(Web Server issue):W435–9.
83. Korf I. Gene finding in novel genomes. *BMC Bioinformatics.* 2004;5:59.
84. Lomsadze A, Ter-Hovhannisyantsyan V, Chernoff YO, Borodovsky M. Gene identification in novel eukaryotic genomes by self-training algorithm. *Nucleic Acids Res.* 2005;33(20):6494–506.
85. Holt C, Yandell M. MAKER2: an annotation pipeline and genome-database management tool for second-generation genome projects. *BMC Bioinformatics.* 2011;12:491.
86. Haas BJ, Salzberg SL, Zhu W, Pertea M, Allen JE, Orvis J, White O, Buell CR, Wortman JR, Automated eukaryotic gene structure annotation using EvidenceModeler and the Program to Assemble Spliced Alignments. *Genome Biol.* 2008;9:R7.
87. Lagesen K, Hallin P, Rodland EA, Staerfeldt HH, Rognes T, Ussery DW. RNAmmer: consistent and rapid annotation of ribosomal RNA genes. *Nucleic Acids Res.* 2007;35(9):3100–8.
88. R Core Team: R: a language and environment for statistical computing. 2015.
89. Alexa A, Rahnenführer J. topGO: enrichment analysis for Gene Ontology. R package version 2220; 2010.
90. Simão FA, Waterhouse RM, Ioannidis P, Kriventseva EV, Zdobnov EM. BUSCO: assessing genome assembly and annotation completeness with single-copy orthologs. *Bioinformatics.* 2015;31(19):3210–2.
91. Wang Y, Tang H, DeBarry JD, Tan X, Li J, Wang X, Lee TH, Jin H, Marler B, Guo H, et al. MCScanX: a toolkit for detection and evolutionary analysis of gene synteny and collinearity. *Nucleic Acids Res.* 2012;40(7):e49.
92. Emms DM, Kelly S. OrthoFinder: phylogenetic orthology inference for comparative genomics. *Genome Biol.* 2019;20(1):238.
93. Buchfink B, Xie C, Huson DH. Fast and sensitive protein alignment using DIAMOND. *Nat Methods.* 2014;12:59.
94. Keeling PJ, Burki F, Wilcox HM, Allam B, Allen EE, Amaral-Zettler LA, Armbrust EV, Archibald JM, Bharti AK, Bell CJ, et al. The Marine Microbial Eukaryote Transcriptome Sequencing Project (MMETSP): illuminating the functional diversity of eukaryotic life in the oceans through transcriptome sequencing. *PLoS Biol.* 2014;12(6):e1001889.
95. Katoh K, Standley DM. MAFFT multiple sequence alignment software version 7: improvements in performance and usability. *Mol Biol Evol.* 2013;30(4):772–80.
96. Nguyen LT, Schmidt HA, von Haeseler A, Minh BQ. IQ-TREE: a fast and effective stochastic algorithm for estimating maximum-likelihood phylogenies. *Mol Biol Evol.* 2015;32(1):268–74.
97. Kalyaanamoorthy S, Minh BQ, Wong TKF, von Haeseler A, Jermini LS. ModelFinder: fast model selection for accurate phylogenetic estimates. *Nat Methods.* 2017;14(6):587–9.

## Publisher's Note

Springer Nature remains neutral with regard to jurisdictional claims in published maps and institutional affiliations.

**Ready to submit your research? Choose BMC and benefit from:**

- fast, convenient online submission
- thorough peer review by experienced researchers in your field
- rapid publication on acceptance
- support for research data, including large and complex data types
- gold Open Access which fosters wider collaboration and increased citations
- maximum visibility for your research: over 100M website views per year

**At BMC, research is always in progress.**

Learn more [biomedcentral.com/submissions](https://www.biomedcentral.com/submissions)

